



**QUEEN'S  
UNIVERSITY  
BELFAST**

## **Type-I interferons induce lung protease responses following respiratory syncytial virus infection via RIG-I-like receptors**

Foronjy, R. F., Taggart, C. C., Dabo, A. J., Weldon, S., Cummins, N., & Geraghty, P. (2015). Type-I interferons induce lung protease responses following respiratory syncytial virus infection via RIG-I-like receptors. *Mucosal immunology*, 8(1), 161-175. <https://doi.org/10.1038/mi.2014.54>

**Published in:**  
Mucosal immunology

**Document Version:**  
Peer reviewed version

**Queen's University Belfast - Research Portal:**  
[Link to publication record in Queen's University Belfast Research Portal](#)

**Publisher rights**  
© Nature Publishing Group

**General rights**  
Copyright for the publications made accessible via the Queen's University Belfast Research Portal is retained by the author(s) and / or other copyright owners and it is a condition of accessing these publications that users recognise and abide by the legal requirements associated with these rights.

**Take down policy**  
The Research Portal is Queen's institutional repository that provides access to Queen's research output. Every effort has been made to ensure that content in the Research Portal does not infringe any person's rights, or applicable UK laws. If you discover content in the Research Portal that you believe breaches copyright or violates any law, please contact [openaccess@qub.ac.uk](mailto:openaccess@qub.ac.uk).

# **Type I interferons induce lung protease responses following respiratory syncytial virus infection via RIG-I-like receptors**

Robert F. Foronjy, MD<sup>1</sup>, Clifford C. Taggart, PhD<sup>2</sup>, Abdoulaye J. Dabo, MSc<sup>1</sup>, Sinéad Weldon, PhD<sup>2</sup>, Neville Cummins<sup>1</sup> and Patrick Geraghty, PhD<sup>1</sup>

\*Mount Sinai Roosevelt Hospital, Mount Sinai Health System, Division of Pulmonary and Critical Care Medicine, New York, NY, USA; †Centre for Infection and Immunity, School of Medicine, Dentistry and Biomedical Sciences, Queen's University Belfast, Belfast, Northern Ireland, UK

Correspondence: Patrick Geraghty, PhD, Department of Medicine, Mount Sinai Roosevelt Hospital, Mount Sinai Health System, Antenucci Building, 432 West 58th Street, Room 311, New York, NY 10019, USA; Telephone: +1 212 523 7265; E-mail: [pgeraghty@chpnet.org](mailto:pgeraghty@chpnet.org)

**DISCLOSURE.** The authors declare no financial conflicts of interest.

## **ACKNOWLEDGEMENTS**

This work was supported by grants made available to P.G. (Flight Attendant Medical Research Institute (YCSA 113380) and to R.F. (US National Institutes of Health 5R01HL098528-04). The authors would like to thank the James P. Mara Center for Lung Disease of the Pulmonary Division of St. Luke's Roosevelt Hospital for their support and Dr. Edward Eden, Dr. Gerard Turino and Dr. Charles Powell.

Abbreviations: RSV, Respiratory syncytial virus; BALF, bronchoalveolar lavage fluid; SAE, small airway epithelial; MMP, matrix metalloproteinases; retinoic acid-inducible gene-1, RIG-I; melanoma differentiation-associated protein-5, MDA5; mitochondrial antiviral-signaling protein, MAVS

**Keywords:** Viral, Gene Regulation, Protease, Knockout Mice, Lung

## ABSTRACT

The role of proteases in viral infection of the lung is poorly understood. Thus, we examined MMP and cathepsin proteases in respiratory syncytial virus (RSV) infected mouse lungs. RSV induced gene expression for matrix metalloproteinases (MMP) -2, -3, -7, -8, -9, -10, -12, -13, -14, -16, -17, -19, -20, -25, -27, -28 and cathepsins B, C, E, G, H, K, L1, S, W and Z in the airways of FVB/NJ mice. Increased proteases were present in the bronchoalveolar lavage fluid (BALF) and lung tissue during infection. Mitochondrial antiviral-signaling protein (*Mavs*) and *Trif* deficient mice were exposed to RSV. *Mavs* deficient mice had significantly lower expression of airway MMP-2, -3, -7, -8, -9, -10, -12, -13 and -28 and cathepsins C, G, K, S, W and Z. In lung epithelial cells, retinoic acid-inducible gene-1 (RIG-I) was identified as the major RIG-I-like receptor (RLR) required for RSV induced protease expression via MAVS. Overexpression of RIG-I or treatment with IFN- $\beta$  in these cells induced MMP and cathepsin gene and protein expression. The significance of RIG-I protease induction was demonstrated by the fact that inhibiting proteases with batimastat, E64 or ribavirin prevented airway hyperresponsiveness and enhanced viral clearance in RSV infected mice.



## INTRODUCTION

Microbial infections in the airways contribute to tissue remodeling and are also a major factor in exacerbating underlying diseases, which have been associated with cytokine and chemokine release from resident lung cells<sup>1</sup>. A protease/antiprotease imbalance can equally be associated with inflammation and extracellular matrix degradation<sup>2</sup>. Proteases have a number of functional effects that contribute to tissue destruction including tissue remodeling, cleavage of soluble innate factors and activation of receptors. Alternatively, proteases also play a critical role in microbial clearance as neutrophil proteases are critical for microbial killing<sup>3</sup>. However, some proteases may even facilitate viral entry and replication into human cells<sup>4</sup>. Thus, determining how viral infection impacts on protease expression, release and activity and the subsequent protease effects on immune responses and lung microenvironment remain important areas to explore.

Matrix metalloproteinases (MMPs) and cathepsins are clinically important proteases that are elevated in many diseases. MMPs are produced by a wide variety of cell-types, including epithelium, fibroblasts, neutrophils, and macrophages<sup>5</sup>. MMPs act on a variety of non-matrix extracellular proteins, such as cytokines, chemokines, receptors, junctional proteins, and antimicrobial peptides, to mediate a broad range of biological processes, such as repair, immunity, and angiogenesis<sup>5</sup>. Similarly, cathepsins are produced by several cell types and tissues and are known to undergo activation by cytokines<sup>6</sup>. Respiratory syncytial virus (RSV) is a virus frequently reported in infants, the elderly, immunocompromised patients as well as healthy adults<sup>7</sup>. Infection alters protease profiles, with MMP-3 and -10 expression being sensitive to RSV inoculation in nasal

epithelial cells<sup>8</sup> and MMP-3 levels in nasopharyngeal aspirates are associated with RSV disease severity<sup>9</sup>. RSV induces MMP-9 gene expression in human bronchial epithelial cells<sup>10</sup> and MMP-9 and -2 were activated by RSV in BALB/c mouse<sup>11</sup>. Bovine RSV can act synergistically with *Histophilus somni* supernatant to elevate MMP-1 and -3 levels, leading to enhanced collagen breakdown and facilitating viral infection efficiency in bovine alveolar type-2 cells<sup>12</sup>. Therefore, previous studies show that RSV induces several proteases and suggest that RSV-inducible proteases may play a major role in disease progression. Proteases become expressed in response to microbial product stimuli<sup>13</sup> with pathogen recognition receptors playing a major role in protease gene regulation when utilizing microbial mimicking agonists<sup>14, 15</sup>. Pathogen recognition receptors (PRR), such as TLRs and retinoic acid-inducible gene-1 (RIG-I)-like receptors (RLRs), induce major signaling cascades in response to viral stimulation<sup>16</sup>. Both TLR mediated Trif signaling and RLR can modulate similar immune processes to regulate cytokine production<sup>17, 18</sup>. The viral load of RSV correlates with the mRNA levels of the RLR, RIG-I<sup>19</sup>. RIG-I and melanoma differentiation-associated protein 5 (MDA5) activate the mitochondrial antiviral-signaling protein (MAVS) to trigger an antiviral response<sup>20</sup>. However, little is known about the role of PRRs in RSV-induced protease expression; although proteases have been shown to modulate TLR3 and RIG-I signaling<sup>21</sup> and inhibition of MMP-9 activity in bronchial epithelial cells prevents syncytia formation and blocks RSV multiplication<sup>10</sup>. Therefore, profiling the protease response during RSV infection and characterizing their regulation and role in disease progression may be beneficial for future treatment of RSV infection.

In this study, we investigate MMP and cathepsin expression responses to RSV infection. *In vivo* and *in vitro* approaches were utilized to identify the major regulatory signaling pathways in RSV-induced protease expression. The influence of Trif and MAVS signaling pathways were examined on RSV-induced protease expression, with RLR dependent MAVS signaling observed to play a major role in RSV-induced MMP and cathepsin expression. These findings indicate that viral infections significantly enhance host protease responses, in a type-I interferon dependent mechanism. Furthermore, we show that the RLR pathways are key players in the host protease response to viral infection and inhibition of proteases may be beneficial in clearing RSV from the airways.

## **RESULTS**

### **RSV infection induces MMP and cathepsin expression and activity**

Increased protease levels have been frequently observed in human airway diseases<sup>22</sup> and play a critical role in microbial killing<sup>3</sup>. While it is established that a viral induced host proteases response occurs, when and which proteases are induced in RSV infected lungs is not yet elucidated. Here we show that mice exposed to RSV infection have increased airway collagenase and elastase activity in their BALF (**Figure 1A**). Elastase activity was observed as early as 24 hours post infection. Both elastase and collagenase activity persisted beyond 9 days post RSV challenge. Protease activity mimicked the RSV N copy number and viral titer within the lung tissue, with reduced protease activity observed upon RSV clearance (**Figure 1B**). RSV infected mice also lost weight during infection

(**Figure 1C**) and had increased BALF immune cell infiltration (**Figure 1D**). Not surprisingly, RSV infection resulted in an infiltration of macrophages, neutrophils and lymphocytes into the lung (**Figure 1D-E**).

The influence of viral infection on protease expression was investigated in greater detail via qPCR by examining the MMP and cathepsin families of proteases. Mice infected with RSV have significant gene expression increases for MMP-2, -3, -7, -8, -9, -10, -12, -13, -14, -16, -17, -19, -20, -25, -27 and -28 (**Figure 2A-H**). Additionally, cathepsins B, C, E, G, H, K, L1, S, W and Z were all enhanced by RSV infection (**Figure 2I-M**). Of note, 9 days post RSV lung infection MMPs -2, -8, -9, -10, -12, -13, -14, -16, -19, -25, -27, -28 and cathepsins E, G, K, L1, S, W and Z remained significantly increased in RSV infected lungs (**Figure 2**). Protein analysis was performed to confirm qPCR data. As illustrated in Figure 3, RSV infection enhanced BALF and lung tissue MMP and cathepsin protein levels and activity. MMP-2, -3, -8, -9 and -12 BALF protein levels were quantified by multiplex analysis (**Figure 3A**). RSV infection increased BALF gelatinase activity, which demonstrated an early MMP-9 response and a later MMP-2 response to RSV challenge (**Figure 3B**). Western blot on lung tissue confirmed that RSV exposure increased cathepsin E, S, G, K, B, W and Z levels 7 days post infection (**Figure 3C**). Cathepsin B, G and S activity levels were elevated in BALF from RSV infected mice (**Figure 3D**).

### **RSV induces the MAVS/MDA5/RIG-I/TLR3 pathways in mouse lungs**

RSV increased protein levels of MDA5, RIG-I, MAVS, MyD88 and Trif (**Figure 4A**). Additionally, phosphorylation of IRF3 and TBK1 were observed following RSV

infection (**Figure 4A**). NF- $\kappa$ B and AP-1 activity were induced by RSV 24 hours post challenge and continued to persist beyond 9 days (**Figure 4B**). As the TLR3/4 and RLR pathways were altered by RSV<sup>19</sup>, *Trif* and *Mavs* KO mice were used to examine the importance of these pathways on protease production *in vivo*. *Mavs* KO mice were utilized as MAVS links RIG-I and MDA5 to antiviral effectors responses. *Trif* KO mice were chosen as both TLR3 and TLR4 are activated by RSV and are the only TLRs that utilize Trif signaling. Mice were exposed to RSV and euthanized every second day until 9 days post RSV challenge. Gene expression studies were performed on days post RSV challenge that corresponded with the maximal level of gene expression for each protease as determined in **Figure 2**. Loss of *Mavs* expression prevented RSV-induced MMP-2, -3, -7, -8, -9, -10, -12, -13 and -28 and cathepsins C, G, K, S, W and Z gene expression (**Figure 5**). Loss of *Trif* expression altered the RSV induced gene expression of MMP-8, -28 and cathepsins G, K, L1, S and Z (**Figure 5**). Interestingly, *Trif* expression suppressed cathepsin G gene expression (**Figure 5**). Tissue and BALF protein analysis confirm *Trif* or *Mavs* regulation of protease expression (**Figure 6A-B**). Loss of *Mavs* impacts on tissue levels of cathepsin E, G, K, S, W and Z (**Figure 6A**) and BALF levels of MMP-2, -3, -8, -9 and -12 (**Figure 6B**). Loss of *Trif* impacted on cathepsin S tissue levels (**Figure 6A**). Additionally, *Trif* and *Mavs* KO mice displayed a similar loss in body weight following RSV infection as wild-type mice (**Figure 6C**) but loss of *Mavs* or *Trif* resulted in a greater viral load in the airway tissue on day 9 following infection compared to wild-type mice (**Figure 6D**).

### **Type-I interferon responses regulate RSV induced protease expression in human SAE cells**

RSV is known to readily infect the airway epithelium<sup>23</sup> and is detectable in the airways using immunofluorescence (**Figure 7A**). Therefore to confirm our *in vivo* findings and identify which RLR is regulating MAVS induced protease production; human airway epithelial cells were infected with RSV and protease expression profiles analyzed by qPCR (**Figure 7**). Gene expression for MMP-1, -3, -7, -8, -9, -10, 12 and 13 were induced in SAE cells upon RSV infection (**Figure 7B**) but were not observed when RSV was UV-treated (**Supplemental Figure S1A**). Multiplex analysis demonstrated that increased MMP-1, -3, -7, -8, -9, -10 and -13 were observed in the media of RSV infected cells (**Figure 7C**). Only cathepsins E and G were induced in SAE cells upon RSV infection (**Figure 7D** and **Supplemental Figure S1B**). Interestingly, using an immunofluorescence approach, only cells positive for RSV antigen had increased MMP-9 and cathepsin E (**Figure 7E**). The tissue inhibitors of metalloproteinases (TIMPs)-1, -2 and -3 were unaltered by RSV stimuli in SAE cells, as observed in the media from SAE cells (**Supplemental Figure S2**).

Since RSV induced a wide range of the proteases in a similar manner to that observed *in vivo*, SAE cells were transfected with siRNA for Trif, MDA5, RIG-I, LGP2 and MAVS (see **Supplemental Figure S3** for siRNA transfection efficiency) to confirm the *in vivo* data but also to determine the RLR responsible for this protease induction. Several of the siRNAs altered protease expression, however RIG-I and MAVS expression were critical for the majority of RSV-induced proteases (**Table 1**). This is of interest as RSV viral load correlates with RIG-I mRNA levels in a study of bronchiolitis in infants<sup>19</sup>. In fact, overexpression of RIG-I in SAE cells up-regulated the same proteases as RSV

stimulation (**Figure 8**). Therefore, these results show that RLRs, such as RIG-I, plays a major role in RSV-mediated protease expression.

As RIG-I signaling regulates RSV-induced protease expression, type-I interferon stimulus was examined for induction of protease expression. SAE cells treated with 1000 units of recombinant human IFN- $\beta$  lead to gene expression induction of the same proteases seen in RSV stimulation (**Figure 8C-D**). Equally, silencing the interferon- $\alpha/\beta$  receptors (IFNAR1 and 2) moderately subdued RSV from inducing gene expression of MMPs and cathepsins (**Figure 8E**). Therefore RSV induced protease expressions are in part an indirect effect of elaborated cytokines, such as a type-I interferon response.

#### **Inhibition of protease activity enhanced RSV clearance from the airways**

Protease inhibitors were utilized *in vivo* to assess the functional role of enhanced proteases in the airways during RSV infection. Wild-type animals were administered a MMP inhibitor (batimastat) or cathepsin inhibitor (E64) daily during RSV infection. Batimastat, a potent inhibitor of MMP -1, -2, -3, -7 and -9, and E64, an effective cysteine protease inhibitor, were intraperitoneal (IP) administered daily. An anti-viral drug, ribavirin, was also administered to a group of animals as ribavirin is administered to patients with severe RSV infection. Also, ribavirin can inhibit MMP-9 activity in THP-1 cells<sup>24</sup>. Animals were euthanized 7 days post RSV challenge and all measurements are on this day. *In vivo* administration of batimastat and E64 significantly inhibited protease activity in the airways (**Figure 9A-B**). Interestingly, ribavirin treatment prevented protease activity in mouse airways during RSV infection (**Figure 9A-B**). This inhibition was comparable to both the protease inhibitors. Animals receiving a protease inhibitor or ribavirin did not lose weight during the week of infection and demonstrated faster

clearance of RSV from the airways (**Figure 9C-D**). Surprisingly, there were reduced immune cells recruited to the airways in animals receiving protease inhibitor or ribavirin (**Figure 9D**). Inhibition of proteases also subdued RSV induced airway hyperresponsiveness, demonstrated by respiratory system resistance (Rrs) measurements during a methacholine dose challenge (**Figure 9E**). IL-4 plays a major role in allergic response to RSV infection resulting in the development of airway hyperresponsiveness and lung eosinophilia<sup>25</sup>. Animals receiving a protease inhibitor or ribavirin had reduced IL-4 responses to RSV (**Figure 9F**), which may contribute to the changes in airway hyperresponsiveness to RSV. IFN- $\beta$  levels were unaltered in all animal groups infected with RSV (**Figure 9F**).

## DISCUSSION

Several studies have investigated the induction of proteases by RSV as early as 1999<sup>26</sup> but the role of these protease families in disease severity and viral clearance has not been established. We characterized how two families of proteases respond to RSV infection and demonstrate that the induction of proteases by RSV is primarily regulated by RLRs, such as RIG-I, in a type-I dependent manner. Prior to this study, RSV infections were known to induce proteases, such as neutrophil elastase<sup>26</sup> and MMP-9<sup>11</sup>, but little was known about the influence of RSV infection on protease expression and the subsequent impact on the lung. We demonstrated that RSV induces expression of protease networks that contribute to disease progression. This study highlights the impact of RSV infection on the proteolytic response within the airways and the potential to target proteases to treat RSV infection.



Prior to undertaking this study, we believed that RSV induced proteases were enhanced via a TLR3/Trif dependent manner, as polyinosinic-polycytidylic acid (poly(i:c)), a synthetic analog of double-stranded RNA (dsRNA), enhanced several MMPs<sup>14, 15</sup> and TLR3/Trif are significantly induced by RSV. However, TLR3/Trif only partially regulated the protease response and RIG-I exerted a far more substantial effect on airway proteases responses. RLRs largely recognizes dsRNA, which is produced during the replication of many viruses<sup>27</sup>. Sendai virus defective interfering (DI) RNA<sup>28</sup> and the genomic “panhandle” structure of influenza virus<sup>29</sup> activate RLR signaling. It has been speculated that these “panhandle” structures allow negative-strand RNA viral genomes to achieve partially double-stranded RNA<sup>30</sup>. Exactly how RNA triggers the RLR pathway for most RNA viruses, including RSV, has yet to be identified. In rhinovirus studies, the bronchial epithelium anti-viral response initially requires recognition of rhinovirus infection by TLR3/TRIF and a subsequent RNA helicases response<sup>16</sup>, suggesting a contribution of both pathways. Indeed, RSV-induced TLR3 is regulated by RIG-I-dependent IFN- $\beta$  that is mediated by both IFN response-stimulated element (ISRE) and signal transducer and activator of transcription (STAT) sites in its proximal promoter<sup>32</sup>. In this manner, TLR3 does not affect RSV-induced NF- $\kappa$ B binding<sup>32</sup>, which may alter the regulation of certain proteases. RIG-I regulated IFN- $\beta$  secretions from infected cells could lead to the Trif activation observed here and the IFNAR1 and 2 receptor induction, which represent two plausible and distinct mechanisms to induce protease production. Therefore, MAVS not only links RIG-I and MDA5 to antiviral effector responses, MAVS can also regulate the RIG-I inducible proteases response to RSV observed in this study.

Recently, investigators have identified several proteases associated with RSV infection, such as MMP-2, -3, -9 and -10<sup>8-11</sup>. We have identified that RSV enhances MMP-2, -3, -7, -8, -9, -10, -12, -13, -14, -16, -17, -19, -20, -25, -27, -28 and cathepsins B, C, E, G, H, K, L1, S, W and Z levels in mouse airways. Whether all of these proteases are present in human viral exacerbations or contribute to disease progression is not yet known but each protease represents many potential future topics of interest. Also it should be noted that RSV gave a robust MMP-1 induction in SAE cells, which could not be evaluated *in vivo*, as mice express no MMP-1. Indeed the protease profile in mice and epithelial cells differed with expression for MMP-2, -14, -17, -20, -25, -27, -28 and cathepsins B, C, H, L1, S, W and Z but its is not surprising as other residential cells or infiltrated immune cells could also contribute to protease production in response to RSV. The functional role of proteases in airway remodeling is well documented<sup>5</sup> but the impact of so many proteases on the microenvironment of the lung is unclear. Our data demonstrates that inhibition of protease activity aids in viral clearance and others have demonstrated that inhibition of MMP-9 activity prevents syncytia formation and blocks RSV multiplication<sup>10</sup>, which suggests resolving the select protease activity in RSV infection is beneficial. These data strengthen the case for the use of protease inhibitors to treat RSV infections. Identifying the exact protease(s) responsible for aiding viral infectivity represents a major future area of investigation. Ribavirin administration to mice prevented the activity of proteases but also gene expression of several proteases, including MMP-9, -10, -12 and cathepsins B, C and S (**Figure S4**). Expression of MMP-9 represents the most likely candidate for the changes in the phenotype observed in our

study as MMP-9 KO mice have reduced airway hyperresponsiveness<sup>33</sup> and inhibition of MMP-9 blocks RSV<sup>10</sup> and fellow Paramyxoviruses, Sendai virus<sup>34</sup>.

Other viruses have been documented to induce protease responses. Indeed, the induction of MMP-9 by Influenza A virus was associated with severe lung pathology in mice<sup>35</sup> and the regulation of neutrophil migration<sup>36</sup>. Also, MMP-9 is higher in children with mumps meningitis<sup>37</sup>. Sendai virus increases MMP-9 activity to drive pneumonia progression by enhancing virus multiplication and aids in the destruction of lung matrix in rats<sup>34</sup>. Whether other viruses lead to the induction of similar host proteases as RSV or play a similar role in disease progression is a major topic for discussion. Our *in vitro* RIG-I overexpression experiment suggests that multiple viruses, which trigger a RIG-I response, may observe a similar protease response. Also, poly(i:c) triggers the expression of multiple MMPs<sup>15</sup>, which further suggests the potential for similar mechanistic protease induction. Other PRRs ligands can induce expression of proteases, such as LPS induction of MMP-1<sup>14, 15</sup> or multiple TLR ligands induction of MMP-9 expression<sup>14</sup>. Therefore, the protease profile induced by other microorganisms and the role of subsequent induced proteases in disease progression remains an intriguing area for future study. RSV could also induce many other proteases outside of the MMP and cathepsin families. Neutrophil elastase has been documented to be elevated in the upper airways of infants infected with RSV<sup>26</sup>. Similarly, we observed increased elastase activity following RSV infection, which may not only be due to increased MMP-12. Interestingly RSV does induce ADAM17 in mouse airways (**Supplemental Figure S5A**). RSV induction of membrane localized ADAM protease activity has been linked to the activation of ERK and IL-8 production in a EGFR dependent manner<sup>38</sup>. In our *in vitro* models RSV also induced

emmprin, an inducer of MMP synthesis (**Supplemental Figure S5B**). Emmprin expression affects the production of MMPs<sup>39</sup> and its expression has been linked to pulmonary fibrosis progression<sup>40</sup> and may contribute to the signaling outlined in this study. Therefore it is conceivable that other families of proteases may also become induced in viral infections and lead to the induction of multiple signaling pathways, which would represent an area that merits further investigation.

Neutrophil derived proteases play an important role in micro-flora clearance, with mice deficient in neutrophil-granule proteases unable to resist staphylococcal and candidal infections<sup>3</sup>. However little is known about the antimicrobial functions of protease networks, especially with viral infection. Prior to this study it was unclear whether the host protease response was required to clear the microbial infection or whether the protease release would have an overall negative impact on lung inflammation and remodeling. Due to the numerous proteases induced by RSV, it is out of the scope of this manuscript to investigate the functional role of each protease in response to RSV but through the use of broad-spectrum protease inhibitors we have determined the impact of proteases on RSV infection and airway hyperresponsiveness to metacholine challenge. Further work is required to determine whether the inhibition of IL-4 by protease inhibitors is the primary impact on preventing RSV induced airway hyperresponsiveness by protease inhibitors or ribavirin. As IL-4 plays a major role in allergic response to RSV infection through the development of airway hyperresponsiveness and lung eosinophilia<sup>25</sup>, it is conceivable that protease regulation of IL-4 may play a major role in disease symptoms. The beneficial effects of inhibiting cathepsins was surprising as cathepsin activity regulates TLR9 interaction with CpG, thereby regulating TLR9

immunity<sup>41</sup>. However recent evidence suggests that cathepsin S can lead to the formation of soluble TLR9 that inhibits TLR9 signaling<sup>42</sup>. Cathepsin S activity was inhibited by E64 and ribavirin. In fact, ribavirin inhibited cathepsin S gene expression. Recent studies suggest that several of the proteases highlighted in this study could contribute to macrophage migration, invasion, differentiation and maturation, such as MMP-10<sup>43</sup>, MMP-19<sup>44</sup> and MMP-28<sup>45</sup>. However, further studies are required to investigate their functional roles here.

In summary, our studies demonstrate that RSV acts in a RLR dependent manner, most likely via RIG-I signaling via type-I IFN, to augment airway protease responses in the lung. Inhibition of protease activity prevented RSV induced airway hyperresponsiveness and lead to enhance clearance of the virus. These findings provide important new insights into the elaborate network of proteases triggered by RSV lung infection.

## **METHODS**

**RSV culture.** Human RSV strain A2 (ATCC, Manassas, VA; #VR-1540) was cultured and virus titers quantified in Hep2 cells by performing plaque assays, as previously described<sup>1</sup>. Briefly, the virus was allowed to grow for 5 days at 37°C in a 5% CO<sub>2</sub> atmosphere. The infected Hep2 monolayers were collected and the virus was released by sonication. Cell debris was removed by centrifugation at 2,500 x g for 5 minutes at 4°C. Virus was collected by centrifuging the supernatant for 2 hours at 22,000 x g at 4°C. Virus were suspended in culture media and snap frozen and maintained at -80°C. Non-

infected Hep2 cell cultures were processed in the same manner as RSV infected cells and the resulting sample collection was used as a mock control.

**Animal models.** *Trif* (*Ticam1*) and *Mavs* knockout (KO) mice were purchased from the Jackson Laboratory (Bar Harbor, ME) and breed on to a FVB/NJ background at least 6 generations. All mice were maintained in a specific pathogen-free facility at Mount Sinai Roosevelt's Hospital. 8-week-old mice were used at the initiation point for all experiments and each experimental parameter had 12 animals per group. Mice were anesthetized by intraperitoneal injection of a mixture of ketamine and xylazine. Animals were intranasally administered  $1 \times 10^6$  plaque forming units (pfu) of RSV or mock. Mock and RSV infection animals were euthanized every second day up to 9 days post challenge. Animals were weighed daily. BALF and lung tissue were collected for analysis of protease levels. Immune cell counts were determined by microscopy and cell type determined by quick diff staining. All animal experiments were performed with approval from Mount Sinai Roosevelt's Hospital Center's Institutional Animal Care and Use Committee approval at Mount Sinai School of Medicine.

**Lung titers and RSV N copy number.** Lungs of infected mice were excised and homogenized using a mechanical homogenizer (Kinematica, Bohemia, NY, USA). The viral titers in the homogenates were quantified by plaque assay on Hep2 cells, as previously described<sup>1</sup>. The concentration of RSV N (pg) was determined by PCR based on a standard curve. The following primers were used at 100 pmol each: 5'-TGG GAG AGG TAG CTC CAG AA-3' and 5'-AGA ATC TGT CCC CTG CTG CTA-3'. Ct was plotted against known RSV standards. Results are represented as natural log pico grams (pg).

**Cell culture.** Monolayers of human SAE cells from healthy subjects (Lonza, Walkersville, MD) were submerged cultured. All cells are assayed and test negative for HIV-1, mycoplasma, Hepatitis-B, Hepatitis-C, bacteria, yeast and fungi upon isolation by Lonza. Cells were only used for experiments at passages 3-6 and at a confluency of approximately 70%. SAE cells were transfected by administering silencing RNA (siRNA) for MDA-5, RIG-I, Trif, MAVS, LGP2, IFNAR1, IFNAR2 or control siRNA (Qiagen, Gaithersburg, MD). Cells were treated with RSV at a MOI of 0.3 for 24 hours. Cells were also treated with mock control as described above. Additionally, SAE cells were transfected with either an empty vector (Origene, Rockville, MD; pCMV6-Entry) or with the same vector that overexpresses *RIG-I* (*DDX58*) as recommended by the manufacturers (Origene). Human recombinant IFN- $\beta$  protein (EMD Millipore) was administered to SAE cells at 1000 Units (U) cells for 24 hours.

**MMP and cathepsin measurements.** MMP and cathepsin gene expression was performed by quantitative PCR (qPCR) using validated Taqman probes (Life Technologies/Applied Biosystems, Carlsbad, CA). All qPCR results are represented as relative quantification (RQ) compared to the mock treated animals and corrected to actin levels. Several MMP levels were measured in BALF and cell culture supernatants using a bead assay (MILLIPLEX MAP MMP Magnetic Bead Panels, EMD Millipore, Billerica, MA) with the BioRad Bio-Plex 200 system (BioRad, Hercules, CA). Cathepsin tissue levels were determined by immunoblots and BALF cathepsin S and B activity assays as previously described<sup>46</sup>. Cathepsin G BALF activity was determined by a commercial available colorimetric assay (Abcam; ab126780). BALF collagenase activity was determined by a colorimetric ninhydrin method, as previously described<sup>22</sup>. Proteinase

activity was also assessed with the same colorimetric ninhydrin method but utilizing casein as the substrate. BALF elastase activity was measured by the hydrolysis of N-succinyl-L-Ala-L-Ala-L-Ala-p-nitroanilide(Suc Ala<sub>3</sub>NA) per minute at 25°C and pH 8.0. BALF gelatinase activity was determined by gelatin zymography.

**Intracellular signaling.** Lung tissue protein from mice was homogenized in radio-immunoprecipitation assay (RIPA) buffer, centrifuged at 13,000 x g for 10 minutes and supernatants collected. Immunoblots were conducted to determine levels of cathepsin E, S, G, K, B, W, Z (all cathepsin antibodies from Santa Cruz Biotechnology, Paso Robles, CA), MDA5, RIG-I, MAVS, Trif, MyD88, p-IRF3(Ser396), IRF3, p-TBK1(Ser172), TBK1/NAK and actin (all remaining antibodies from Cell Signaling Technologies, Danvers, MA). Chemiluminescence detection was performed using the Bio-Rad Laboratories Molecular Imager ChemiDoc XRS+ imaging system. Densitometry was performed on each target and represented as a ratio of pixel intensity compared to actin, using Bio-Rad Laboratories Image Lab software (version 4.0, build 16). NF-κBp65 and AP-1 levels were measured on the nuclear protein extracts using specific activation assays from Active Motif (46096 and 40096; Active Motif, Carlsbad, CA, USA). Relative transcription factor activity is represented as a percentage compared to the mock treated group.

**Immunofluorescence.** Immunoreactivity assays were performed on SAE cells with polyclonal anti-RSV (Abcam; ab20745), anti-MMP9 (Cell signaling Technologies; # 2270) and anti-cathepsin E (Santa Cruz biotechnologies; sc-166343) antibodies. Mouse lung tissue was also examined for RSV immunoreactivity.



**Airway responses to methacholine challenge.** Airway responses to methacholine (Sigma Chemical, St. Louis, MO) were assessed with the Scireq Flexivent system (Scireq, Montreal, QC, Canada) at 1-week post RSV challenge and daily intraperitoneally (IP) injections of vehicle (20% DMSO), 60 mg/Kg batimastat, 5 mg/Kg E64 or 30 mg/Kg ribavirin. Animals were anesthetized with ketamine/xylazine (10 mg/kg) and paralysis was induced with 1 mg/kg pancuronium bromide IP (Sigma). The linear single-compartment model was used to assess total respiratory system resistance (Rrs). Methacholine dose responses were determined.

**Statistical analyses.** For statistical analysis, data from 12 animals or multiple separate cell experiments were pooled. Data are expressed as means  $\pm$  S.E.M. Differences between groups of mice over time were compared by two-way analysis of variance (ANOVA). Individual differences between groups were tested by multiple comparison and analysis using the Bonferroni post-test. Pairs of groups were compared by Student's t test (two tailed). p values for significance were set at 0.05. All analysis was performed using GraphPad Prism Software (Version 5 for Mac OS X).

**SUPPLEMENTARY MATERIAL** is linked to the online version of the paper at <http://www.nature.com/mi>

## REFERENCES

1. Foronjy RF, Dabo AJ, Taggart CC, Weldon S, Geraghty P. Respiratory syncytial virus infections enhance cigarette smoke induced COPD in mice. *PLoS One* 2014; **9**(2): e90567.
2. Foronjy R, Nkyimbeng T, Wallace A, Thankachen J, Okada Y, Lemaitre V *et al.* Transgenic expression of matrix metalloproteinase-9 causes adult-onset

- emphysema in mice associated with the loss of alveolar elastin. *Am J Physiol Lung Cell Mol Physiol* 2008; **294**(6): L1149-1157.
3. Reeves EP, Lu H, Jacobs HL, Messina CG, Bolsover S, Gabella G *et al.* Killing activity of neutrophils is mediated through activation of proteases by K<sup>+</sup> flux. *Nature* 2002; **416**(6878): 291-297.
  4. Kubo Y, Hayashi H, Matsuyama T, Sato H, Yamamoto N. Retrovirus entry by endocytosis and cathepsin proteases. *Adv Virol* 2012; **2012**: 640894.
  5. Shiomi T, Lemaitre V, D'Armiento J, Okada Y. Matrix metalloproteinases, a disintegrin and metalloproteinases, and a disintegrin and metalloproteinases with thrombospondin motifs in non-neoplastic diseases. *Pathol Int* 2010; **60**(7): 477-496.
  6. Zheng T, Zhu Z, Wang Z, Homer RJ, Ma B, Riese RJ, Jr. *et al.* Inducible targeting of IL-13 to the adult lung causes matrix metalloproteinase- and cathepsin-dependent emphysema. *J Clin Invest* 2000; **106**(9): 1081-1093.
  7. Falsey AR, Hennessey PA, Formica MA, Cox C, Walsh EE. Respiratory syncytial virus infection in elderly and high-risk adults. *N Engl J Med* 2005; **352**(17): 1749-1759.
  8. Hirakawa S, Kojima T, Obata K, Okabayashi T, Yokota SI, Nomura K *et al.* Marked induction of matrix metalloproteinase-10 by respiratory syncytial virus infection in human nasal epithelial cells. *J Med Virol* 2013.
  9. Schuurhof A, Bont L, Hodemaekers HM, de Klerk A, de Groot H, Hofland RW *et al.* Proteins involved in extracellular matrix dynamics are associated with respiratory syncytial virus disease severity. *Eur Respir J* 2012; **39**(6): 1475-1481.
  10. Yeo SJ, Yun YJ, Lyu MA, Woo SY, Woo ER, Kim SJ *et al.* Respiratory syncytial virus infection induces matrix metalloproteinase-9 expression in epithelial cells. *Arch Virol* 2002; **147**(2): 229-242.
  11. Li W, Shen HH. Effect of respiratory syncytial virus on the activity of matrix metalloproteinase in mice. *Chin Med J (Engl)* 2007; **120**(1): 5-11.
  12. Agnes JT, Zekarias B, Shao M, Anderson ML, Gershwin LJ, Corbeil LB. Bovine respiratory syncytial virus and *Histophilus somni* interaction at the alveolar barrier. *Infect Immun* 2013; **81**(7): 2592-2597.
  13. Pierce RA, Sandefur S, Doyle GA, Welgus HG. Monocytic cell type-specific transcriptional induction of collagenase. *J Clin Invest* 1996; **97**(8): 1890-1899.

14. Geraghty P, Dabo AJ, D'Armiento J. TLR4 protein contributes to cigarette smoke-induced matrix metalloproteinase-1 (MMP-1) expression in chronic obstructive pulmonary disease. *J Biol Chem* 2011; **286**(34): 30211-30218.
15. Ritter M, Mennerich D, Weith A, Seither P. Characterization of Toll-like receptors in primary lung epithelial cells: strong impact of the TLR3 ligand poly(I:C) on the regulation of Toll-like receptors, adaptor proteins and inflammatory response. *J Inflamm (Lond)* 2005; **2**: 16.
16. Slater L, Bartlett NW, Haas JJ, Zhu J, Message SD, Walton RP *et al.* Co-ordinated role of TLR3, RIG-I and MDA5 in the innate response to rhinovirus in bronchial epithelium. *PLoS Pathog* 2010; **6**(11): e1001178.
17. Marr N, Wang TI, Kam SH, Hu YS, Sharma AA, Lam A *et al.* Attenuation of respiratory syncytial virus-induced and RIG-I-dependent type I IFN responses in human neonates and very young children. *J Immunol* 2014; **192**(3): 948-957.
18. Xie XH, Zang N, Li SM, Wang LJ, Deng Y, He Y *et al.* Resveratrol Inhibits respiratory syncytial virus-induced IL-6 production, decreases viral replication, and downregulates TRIF expression in airway epithelial cells. *Inflammation* 2012; **35**(4): 1392-1401.
19. Scagnolari C, Midulla F, Pierangeli A, Moretti C, Bonci E, Berardi R *et al.* Gene expression of nucleic acid-sensing pattern recognition receptors in children hospitalized for respiratory syncytial virus-associated acute bronchiolitis. *Clin Vaccine Immunol* 2009; **16**(6): 816-823.
20. Hou F, Sun L, Zheng H, Skaug B, Jiang QX, Chen ZJ. MAVS forms functional prion-like aggregates to activate and propagate antiviral innate immune response. *Cell* 2011; **146**(3): 448-461.
21. Qu L, Feng Z, Yamane D, Liang Y, Lanford RE, Li K *et al.* Disruption of TLR3 signaling due to cleavage of TRIF by the hepatitis A virus protease-polymerase processing intermediate, 3CD. *PLoS Pathog* 2011; **7**(9): e1002169.
22. D'Armiento JM, Goldklang MP, Hardigan AA, Geraghty P, Roth MD, Connett JE *et al.* Increased matrix metalloproteinase (MMPs) levels do not predict disease severity or progression in emphysema. *PLoS One* 2013; **8**(2): e56352.
23. Zhang L, Peeples ME, Boucher RC, Collins PL, Pickles RJ. Respiratory syncytial virus infection of human airway epithelial cells is polarized, specific to ciliated cells, and without obvious cytopathology. *J Virol* 2002; **76**(11): 5654-5666.
24. Kennedy A, Hennessy M, Bergin C, Mulcahy F, Hopkins S, Spiers JP. Ribavirin and interferon alter MMP-9 abundance in vitro and in HIV-HCV-coinfected patients. *Antivir Ther* 2011; **16**(8): 1237-1247.

25. Khaitov MR, Shilovskiy IP, Nikonova AA, Shershakova NN, Kamyshnikov OY, Babakhin AA *et al.* siRNAs targeted to IL-4 and RSV reduce airway inflammation in a mouse model of virus-induced asthma exacerbation. *Hum Gene Ther* 2014.
26. Abu-Harb M, Bell F, Finn A, Rao WH, Nixon L, Shale D *et al.* IL-8 and neutrophil elastase levels in the respiratory tract of infants with RSV bronchiolitis. *Eur Respir J* 1999; **14**(1): 139-143.
27. Sun Q, Sun L, Liu HH, Chen X, Seth RB, Forman J *et al.* The specific and essential role of MAVS in antiviral innate immune responses. *Immunity* 2006; **24**(5): 633-642.
28. Martinez-Gil L, Goff PH, Hai R, Garcia-Sastre A, Shaw ML, Palese P. A Sendai virus-derived RNA agonist of RIG-I as a virus vaccine adjuvant. *J Virol* 2013; **87**(3): 1290-1300.
29. Rehwinkel J, Tan CP, Goubau D, Schulz O, Pichlmair A, Bier K *et al.* RIG-I detects viral genomic RNA during negative-strand RNA virus infection. *Cell* 2010; **140**(3): 397-408.
30. Schlee M, Roth A, Hornung V, Hagmann CA, Wimmenauer V, Barchet W *et al.* Recognition of 5' triphosphate by RIG-I helicase requires short blunt double-stranded RNA as contained in panhandle of negative-strand virus. *Immunity* 2009; **31**(1): 25-34.
31. Loo YM, Fornek J, Crochet N, Bajwa G, Perwitasari O, Martinez-Sobrido L *et al.* Distinct RIG-I and MDA5 signaling by RNA viruses in innate immunity. *J Virol* 2008; **82**(1): 335-345.
32. Liu P, Jamaluddin M, Li K, Garofalo RP, Casola A, Brasier AR. Retinoic acid-inducible gene I mediates early antiviral response and Toll-like receptor 3 expression in respiratory syncytial virus-infected airway epithelial cells. *J Virol* 2007; **81**(3): 1401-1411.
33. Cataldo DD, Tournoy KG, Vermaelen K, Munaut C, Foidart JM, Louis R *et al.* Matrix metalloproteinase-9 deficiency impairs cellular infiltration and bronchial hyperresponsiveness during allergen-induced airway inflammation. *Am J Pathol* 2002; **161**(2): 491-498.
34. Yamada H, Le QT, Kousaka A, Higashi Y, Tsukane M, Kido H. Sendai virus infection up-regulates trypsin I and matrix metalloproteinase-9, triggering viral multiplication and matrix degradation in rat lungs and lung L2 cells. *Arch Virol* 2006; **151**(12): 2529-2537.

35. Lee YH, Lai CL, Hsieh SH, Shieh CC, Huang LM, Wu-Hsieh BA. Influenza A virus induction of oxidative stress and MMP-9 is associated with severe lung pathology in a mouse model. *Virus Res* 2013.
36. Bradley LM, Douglass MF, Chatterjee D, Akira S, Baaten BJ. Matrix metalloprotease 9 mediates neutrophil migration into the airways in response to influenza virus-induced toll-like receptor signaling. *PLoS Pathog* 2012; **8**(4): e1002641.
37. Sulik A, Wojtkowska M, Oldak E. Elevated levels of MMP-9 and TIMP-1 in the cerebrospinal fluid of children with echovirus type 30 and mumps meningitis. *Scand J Immunol* 2008; **68**(3): 323-327.
38. Monick MM, Cameron K, Staber J, Powers LS, Yarovinsky TO, Koland JG *et al.* Activation of the epidermal growth factor receptor by respiratory syncytial virus results in increased inflammation and delayed apoptosis. *J Biol Chem* 2005; **280**(3): 2147-2158.
39. Jouneau S, Khorasani N, P DES, Macedo P, Zhu J, Bhavsar PK *et al.* EMMPRIN (CD147) regulation of MMP-9 in bronchial epithelial cells in COPD. *Respirology* 2011; **16**(4): 705-712.
40. Guillot S, Delaval P, Brinchault G, Caulet-Maugendre S, Depince A, Lena H *et al.* Increased extracellular matrix metalloproteinase inducer (EMMPRIN) expression in pulmonary fibrosis. *Exp Lung Res* 2006; **32**(3-4): 81-97.
41. Matsumoto F, Saitoh S, Fukui R, Kobayashi T, Tanimura N, Konno K *et al.* Cathepsins are required for Toll-like receptor 9 responses. *Biochem Biophys Res Commun* 2008; **367**(3): 693-699.
42. Chockalingam A, Cameron JL, Brooks JC, Leifer CA. Negative regulation of signaling by a soluble form of toll-like receptor 9. *Eur J Immunol* 2011; **41**(8): 2176-2184.
43. Murray MY, Birkland TP, Howe JD, Rowan AD, Fidock M, Parks WC *et al.* Macrophage migration and invasion is regulated by MMP10 expression. *PLoS One* 2013; **8**(5): e63555.
44. Beck IM, Ruckert R, Brandt K, Mueller MS, Sadowski T, Brauer R *et al.* MMP19 is essential for T cell development and T cell-mediated cutaneous immune responses. *PLoS One* 2008; **3**(6): e2343.
45. Gharib SA, Johnston LK, Huizar I, Birkland TP, Hanson J, Wang Y *et al.* MMP28 promotes macrophage polarization toward M2 cells and augments pulmonary fibrosis. *J Leukoc Biol* 2013.

46. Geraghty P, Greene CM, O'Mahony M, O'Neill SJ, Taggart CC, McElvaney NG. Secretory leucocyte protease inhibitor inhibits interferon-gamma-induced cathepsin S expression. *J Biol Chem* 2007; **282**(46): 33389-33395.

## FIGURE LEGENDS

**Figure 1** RSV infection induces protease activity in the airways. FVB/NJ mice were infected with  $1 \times 10^6$  pfu of RSV and a group of animals were euthanized at day 0, 1, 3, 5, 7 and 9 post infection. (A) BALF had greater collagenase and elastase activity in animals infected with RSV compared to mock controls. (B) RSV N copy number and viral load were greatest 5 days post RSV challenge and were at the lower level of detection by day 9. (C) RSV infection resulted in a significant drop in body weight in animals and (D) an increase in BALF cellularity. Graphs are represented as mean  $\pm$  S.E.M., where each measurement was performed 3 times on 12 animals/group. \* and \*\* represents a p value less than 0.05 compared to mock treated mice or day 1 RSV treated mice, respectively. p values shown comparing RSV to mock treated mice connected by a line. (E) Representative images of mice lungs from each RSV treated group (scale bar=10  $\mu$ M).

**Figure 2** RSV infection induces MMP and cathepsin gene expression. FVB/NJ mice were infected with  $1 \times 10^6$  pfu of RSV and animals were euthanized every second day as previously described. (A-H) MMP and (I-M) cathepsin lung gene expression were analyzed by qPCR. Graphs are represented as relative quantification (RQ) of the mean  $\pm$  S.E.M, with each measurement performed 3 times on 12 animals/group. \*Represents a p value less than 0.05 compared to mock treated mice on each corresponding day.

**Figure 3** RSV infections induce MMP and cathepsin protein expression and activity. (A) BALF MMP-2, -3, -8, -9 and -12 levels were determined by multiplex analysis on mock

treated and RSV treated animals. (B) Gelatinase activity was analyzed in BALF using gelatin zymography. Bands corresponding to MMP-2 and MMP-9 are highlighted. (C) Cathepsin E, S, G, K, B, W and Z lung protein levels were analyzed by immunoblotting and corresponding densitometry analysis. (D) Cathepsin B, S and G activity levels were determined in BALF. FI represents fluorescent intensity. Graphs are represented as mean  $\pm$  S.E.M, where each measurement was performed 3 times on 12 animals/group. \*Represents a p value less than 0.05 compared to mock treated mice. p values shown, comparing both treatments connected by a line.

**Figure 4** RSV induces the MAVS/MDA5/RIG-I/TLR3 pathways in mouse lungs. (A) Immunoblots were performed to examine levels of MDA, RIG-I, MAVS, MyD88 and TRIF protein and IRF3 and TBK1 phosphorylation in lung tissue of RSV infected animals. Densitometry analysis was performed against actin or total protein (TBK1 and IRF3) levels for all samples from multiple immunoblots. (B) NF $\kappa$ B and AP-1 nuclear activity levels were determined in the lung tissue of mock and RSV treated mice. Graphs are represented as mean  $\pm$  S.E.M, where each measurement performed 3 times on 12 animals/group. \*Represents a p value less than 0.05 compared to mock treated mice on each corresponding day.

**Figure 5** MAVS is required for the gene expression of the majority of RSV inducible airway proteases. Wildtype, *Trif* (*Ticam1*) and *Mavs* KO mice were infected with  $1 \times 10^6$  pfu of RSV and animals were euthanized every second day as previously described. MMP and cathepsin gene expression in lung tissue was analyzed by qPCR on the day post infection with the maximal level of gene expression for each protease, as determined in **Figure 2**. MMP-10 and -20 were examined one-day post infection. MMP-7, -8, -9 and

cathepsin B were examined three days post infection. MMP-3, -16 and -17 were examined five days post infection. MMP-2, -12, -13, -14, -19, -25, -27, -28, cathepsin C, L1, S, W and Z were examined seven days post infection. Cathepsin E, G, H and K were examined nine days post infection. Results are represented as relative quantification (RQ) of the mean  $\pm$  S.E.M when compared to mock treated animals on each corresponding day, with each measurement performed 3 times on 12 animals/group. p values shown, comparing treatments connected by a line.

**Figure 6** MAVS is required for the protein expression of the majority of RSV inducible airway proteases. (A) Immunoblots (Cathepsin E, G, K, S, W, Z, MMP-14, MMP-28 and actin) were performed on lung tissue 7 days post RSV challenge and densitometry analysis was determined. The Y-axis represents densitometry value for all graphs. (B) Multiplex analysis (MMP-2, -3, -8, -9 and -12) was performed on BALF 7 days post RSV challenge. (C) RSV infection resulted in a drop in body weight in all animal groups and (D) a significant increase in the viral load 9 days post RSV challenge in the *Mavs* KO mouse group compared to mock treated mice. Graphs are represented as mean  $\pm$  S.E.M., where each measurement was performed 3 times on 12 animals/group. p values shown, comparing both treatments connected by a line. \*Represents a p value less than 0.05 comparing *Mavs* KO mice to wildtype mice 9 days post RSV challenge.

**Figure 7** The MMP and cathepsin gene expression profile in human SAE cells exposed to RSV. (A) Immunofluorescence was performed on tissue from mock or RSV infected mice 5 days post RSV challenge with an antibody that recognizes RSV antigen (red). (B) MMP gene expression was performed in SAE cells treated for 24 hours with mock or RSV was analyzed by qPCR. (C) MMP-1, -3, -7, -8, -9, -10 and -13 in cell culture



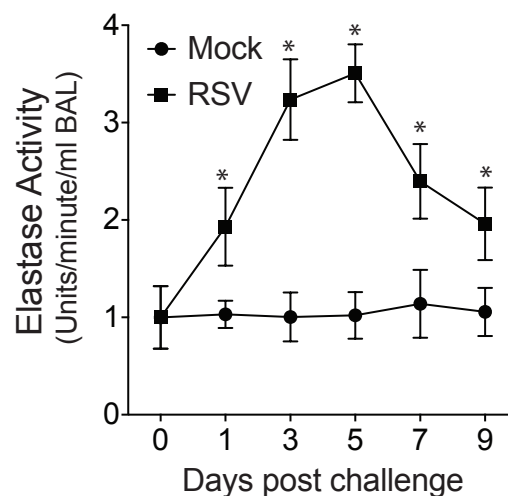
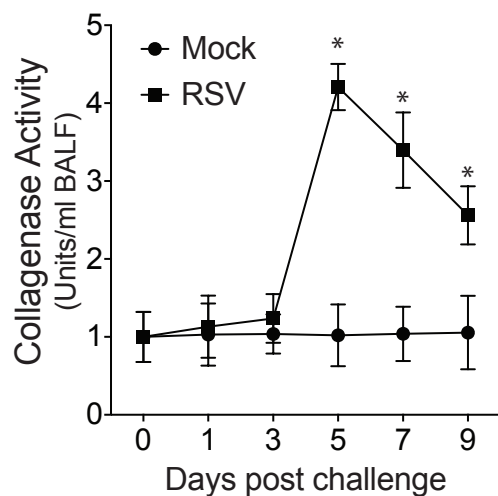
supernatants were determined by multiplex analysis following RSV infection. (D) Cathepsin gene expression was performed in SAE cells treated for 24 hours with mock or RSV was analyzed by qPCR. (B and D) Dotted line represents mock treated level of expression. \*Represents a p value less than 0.05 compared to mock treated mice. (E) Co-immunofluorescence was performed on cells for either MMP-9 or cathepsin E (green) and with an antibody that recognizes RSV antigen (red) (Scale bars are 20  $\mu$ m). Merged images demonstrate co-localization (orange). Graphs are represented as mean  $\pm$  S.E.M, where n=10 per group. p values shown, comparing both treatments connected by a line.

**Figure 8** Overexpression of RIG-I in human SAE cells and IFN- $\beta$  stimulation induces protease expression. (A) MMP and cathepsin gene expression was performed on SAE cells transfected with either an empty vector (pCMV6-Entry) or with the same vector overexpressing *RIG-I* (*DDX58*). Immunoblots were performed to determine RIG-I protein levels compared to actin and three individual transfections are presented. (B) MMP-1, -3, -7, -8, -9, -10 and -13 media levels were determined by multiplex analysis 24 hours following RSV infection. (C) MMP and cathepsin gene expression were determined in SAE cells following treatment with 1000 units of recombinant human IFN- $\beta$  for 24 hours. (D) Supernatant levels of MMP-8, -9, -10 and -13 following IFN- $\beta$  stimulation. (E) MMP and cathepsin gene expression was performed on SAE cells transfected with siRNA for IFNAR1, IFNAR2 or both and treated with RSV. Immunoblots were performed to determine protein silencing compared to actin and two individual transfections are presented. All graphs are represented as mean  $\pm$  S.E.M, where n=10 per group. \*Represents a p value less than 0.05 compared to empty vector-transfected cells.

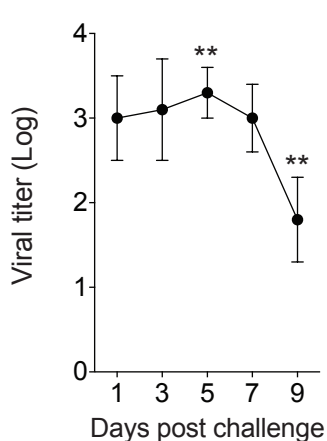
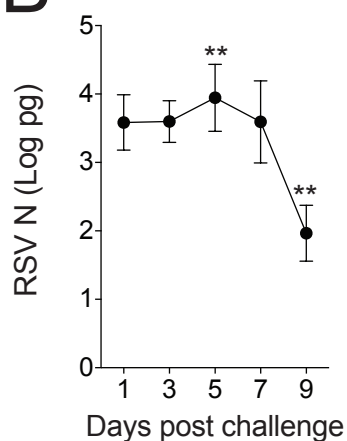
**Figure 9** Administration of protease inhibitors or ribavirin aid in RSV clearance and subdue airway hyperresponsiveness in mice. FVB/NJ mice were injected with vehicle, bastimastat, E64 or ribavirin prior to infected with  $1 \times 10^6$  pfu of RSV and animals received daily following-up injections until they were euthanized at day 7-post infection. BALF (A) collagenase, casein degradation capability, cathepsin S and G elastase activity and (B) gelatinase activity were determined in all animals groups. (C) Animal body weight, (D) BALF cellularity and RSV N copy number were determined in all animals. (E) Airway hyperresponsiveness to increasing doses of methacholine was assessed in each animal group. (F) IL-4 and IFN- $\beta$  gene expression in lung tissue was analyzed by qPCR. Graphs are represented as mean  $\pm$  S.E.M., where each measurement was performed 3 times on 12 animals/group. \* and \*\* represents a p value less than 0.05 compared to mock and vehicle treated mice or RSV and vehicle treated mice, respectively.

# Figure 1

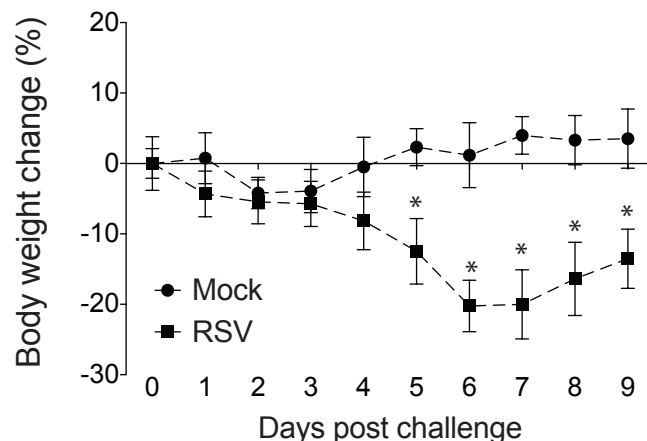
## A



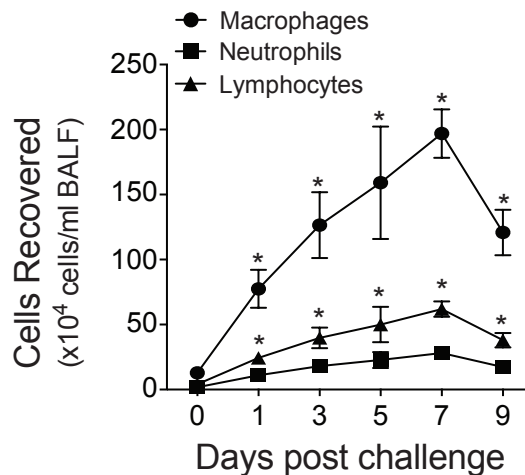
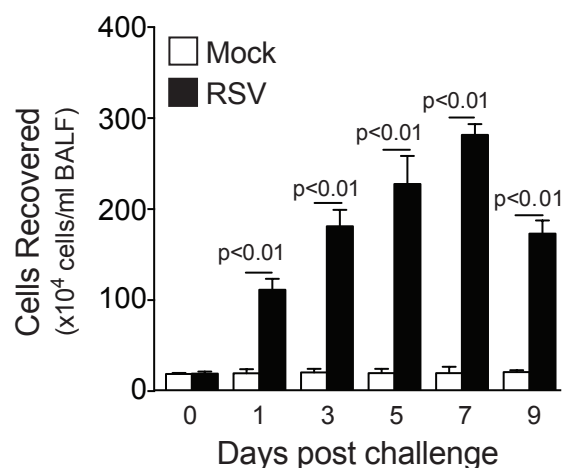
## B



## C



## D



## E

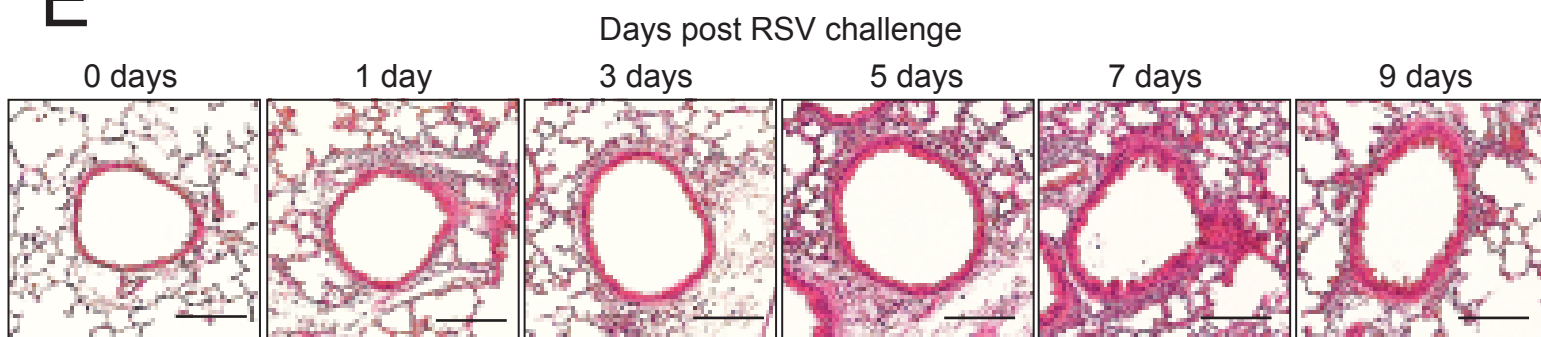


# Figure 2

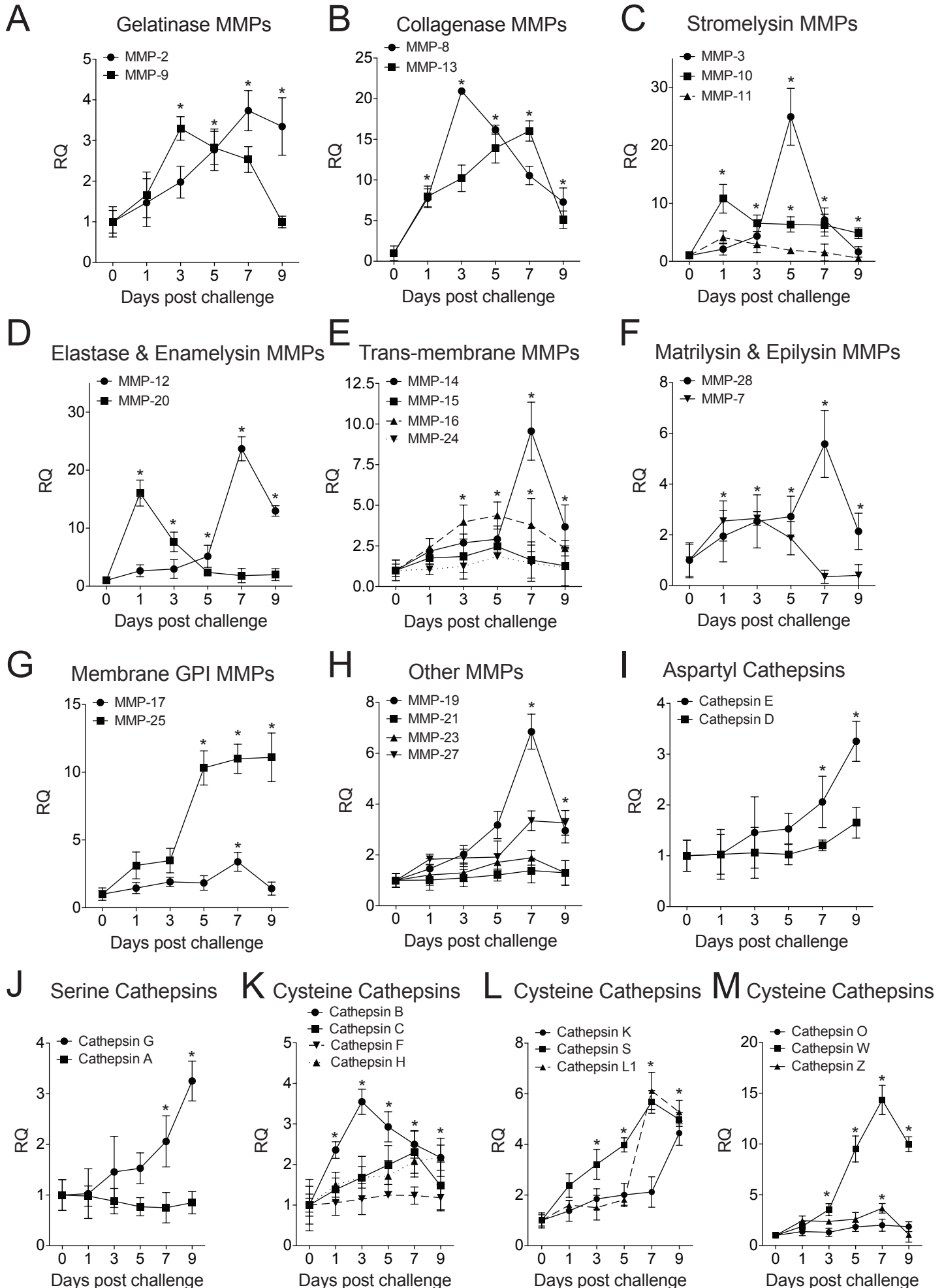
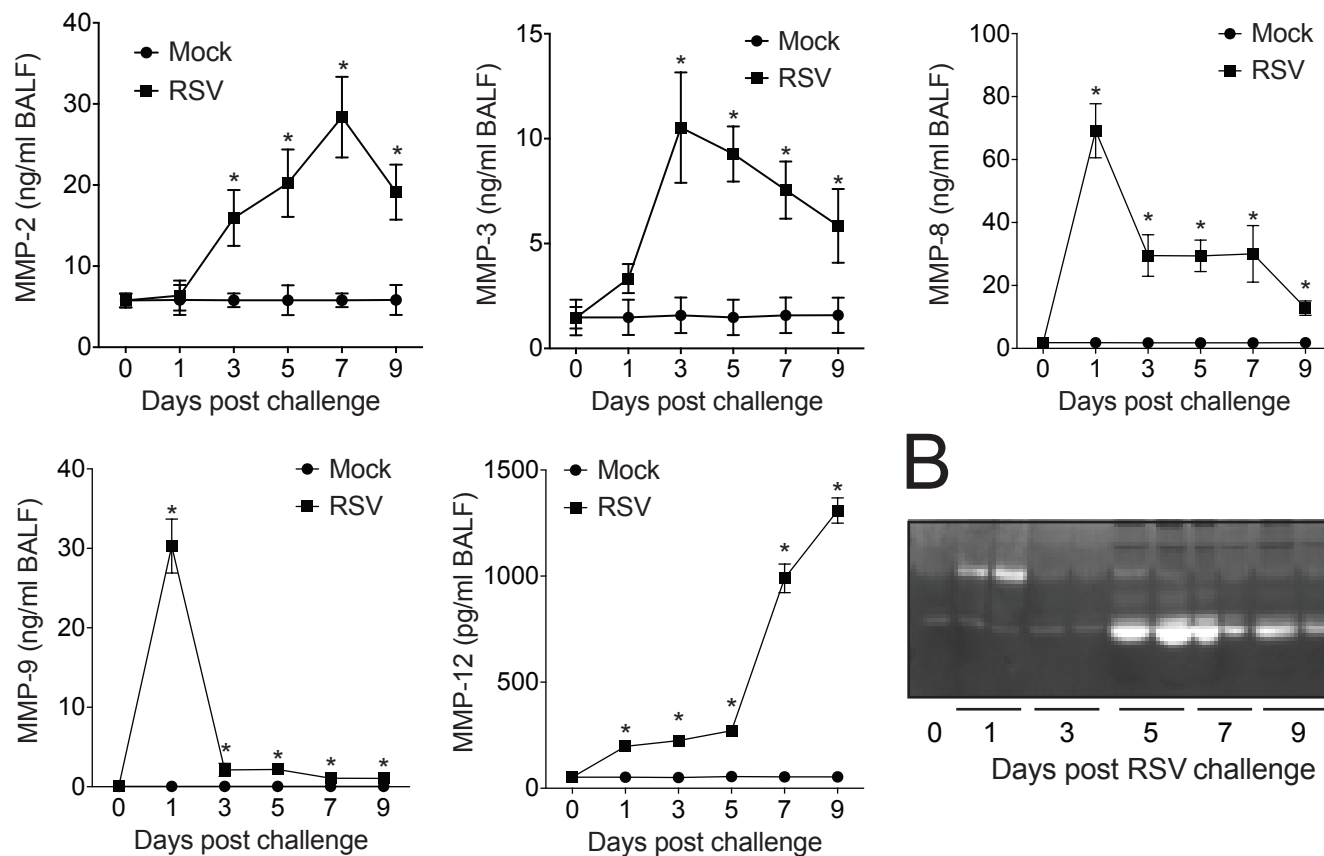
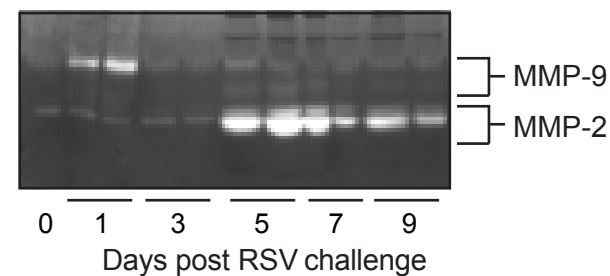


# Figure 3

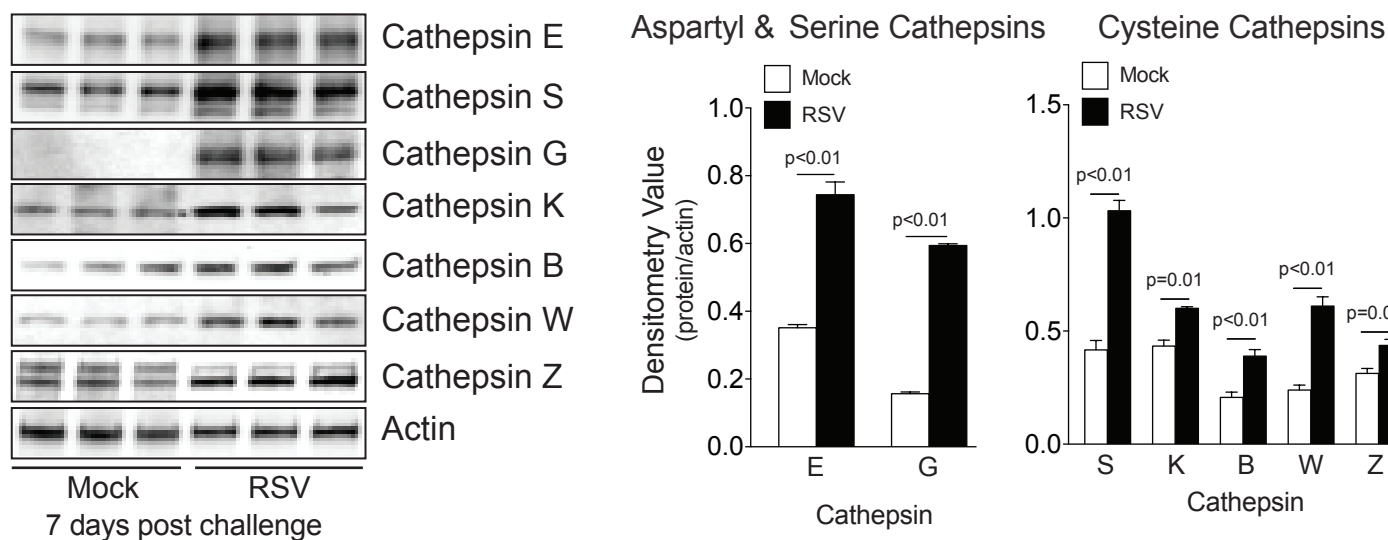
## A



## B



## C



## D

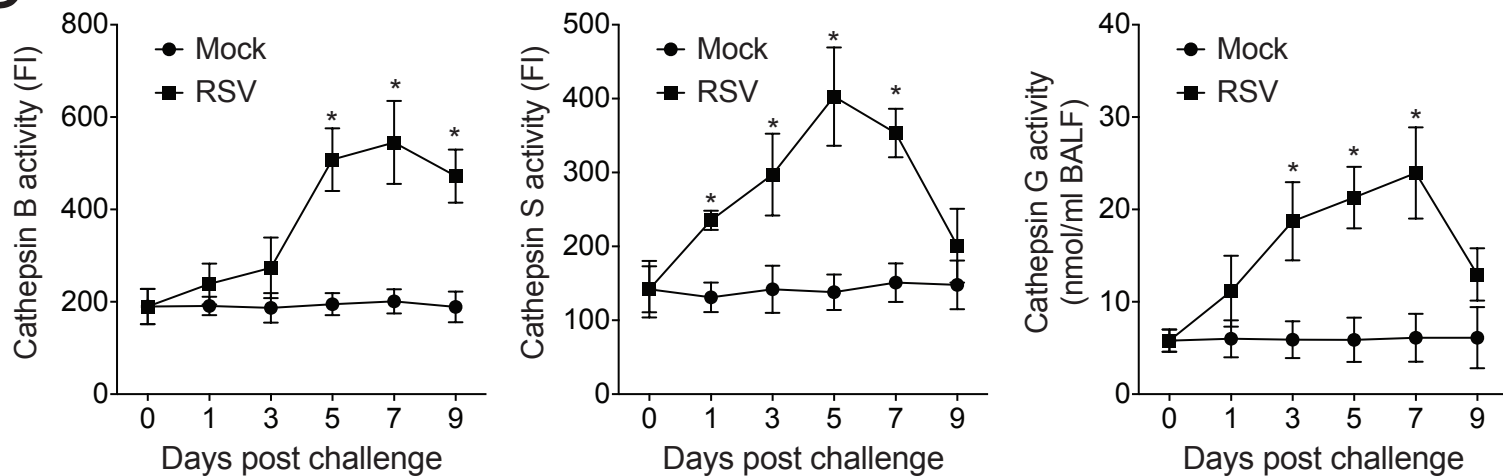
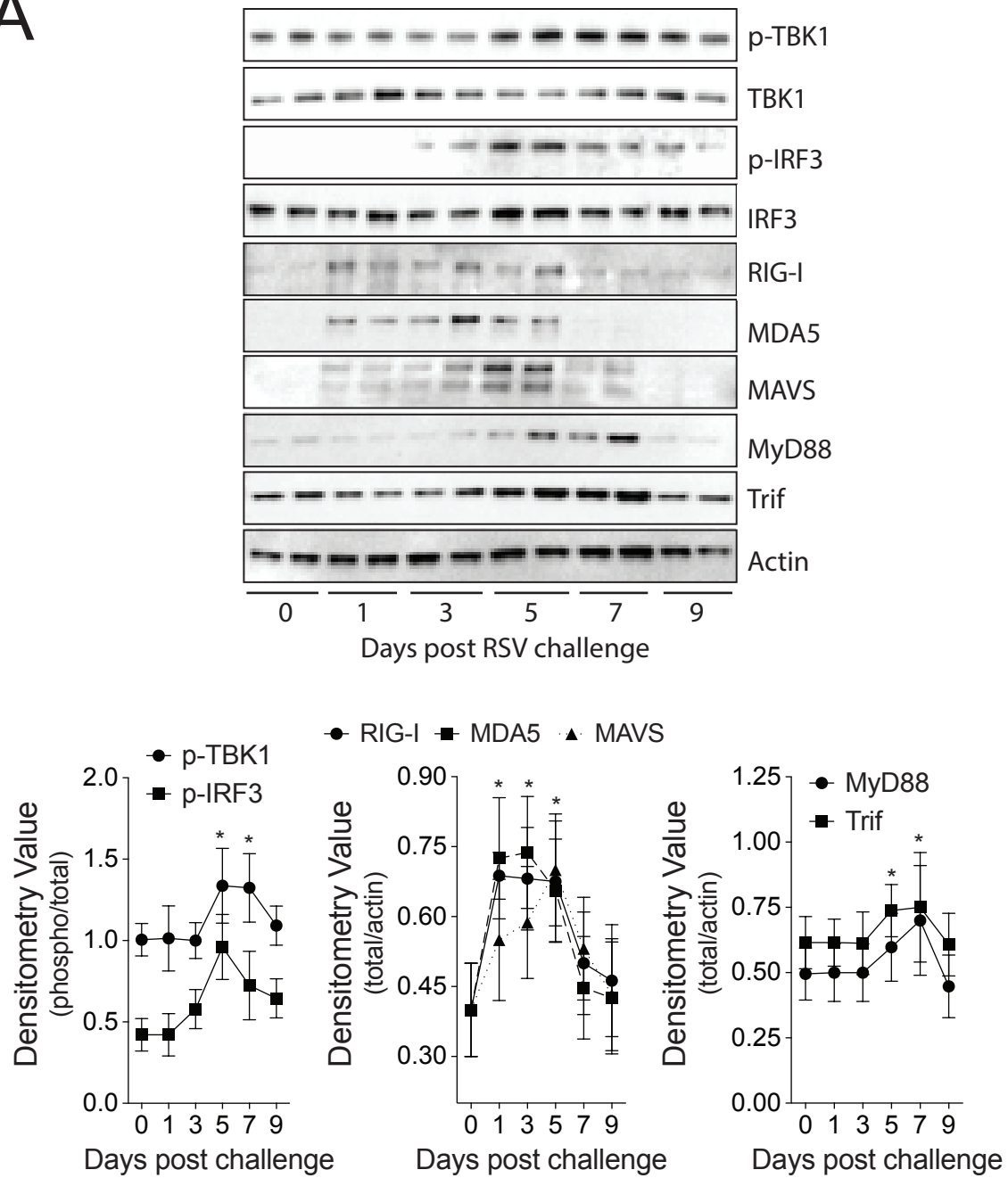
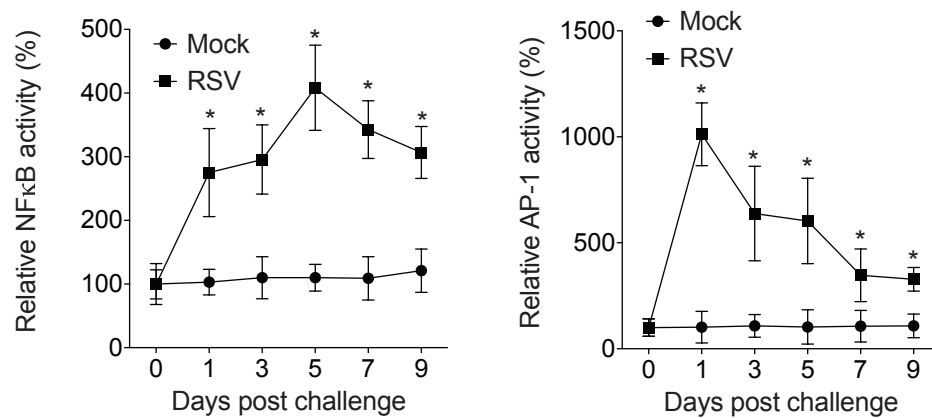


# Figure 4

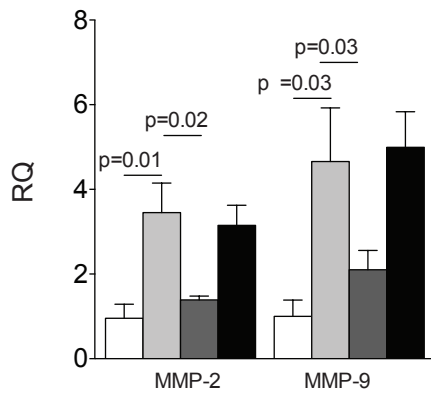
## A



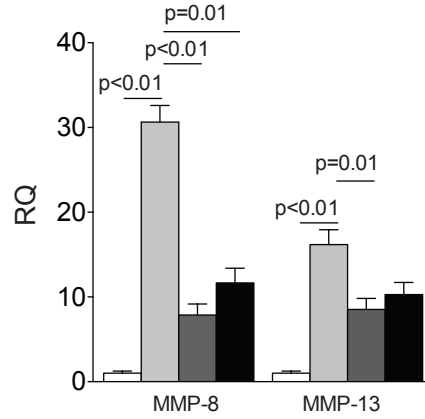
## B



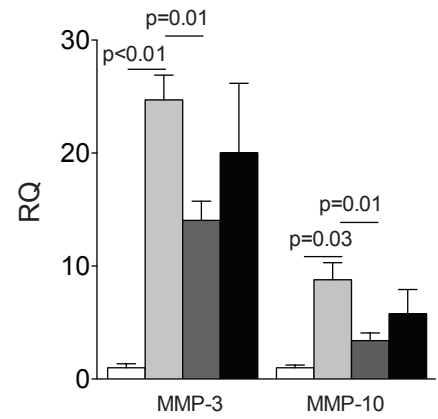
### Gelatinase MMPs



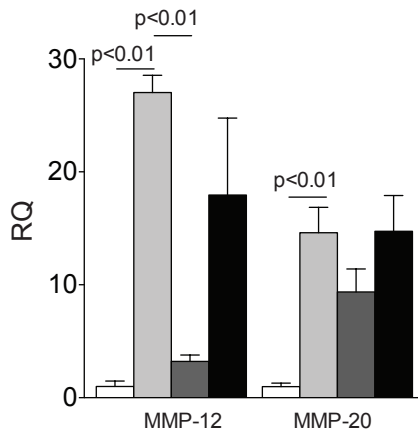
### Collagenase MMPs



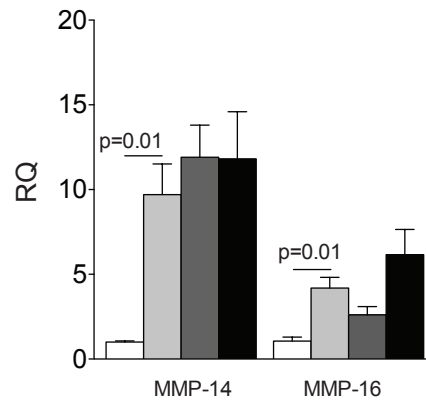
### Stromelysin MMPs



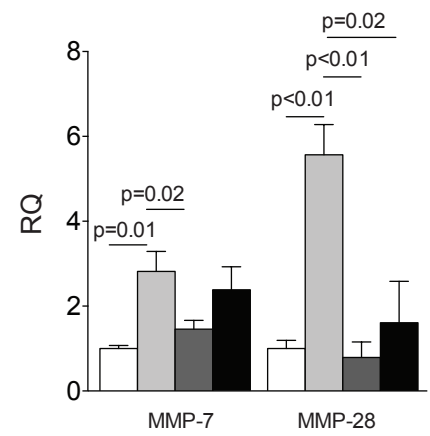
### Elastase & Enamelysin MMPs



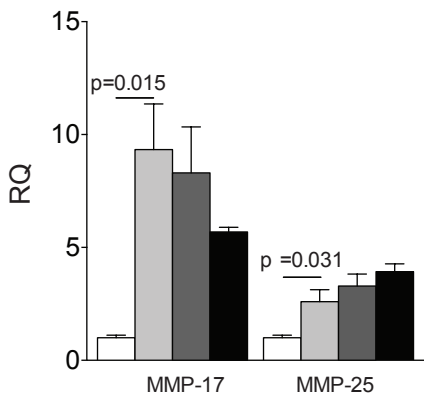
### Trans-membrane MMPs



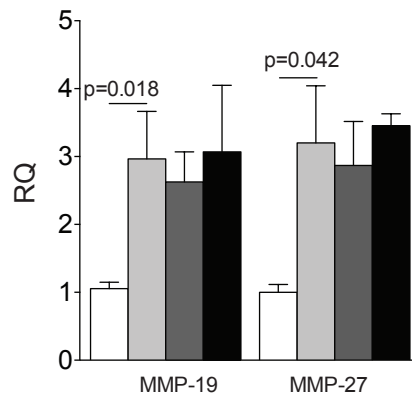
### Matrilysin & Epilysin MMPs



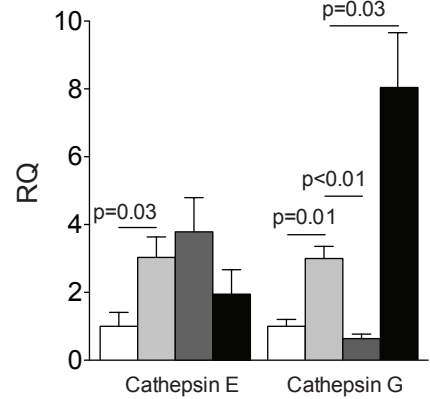
### Membrane GPI MMPs



### Other MMPs



### Aspartyl & Serine Cathepsins



### Cysteine Cathepsins

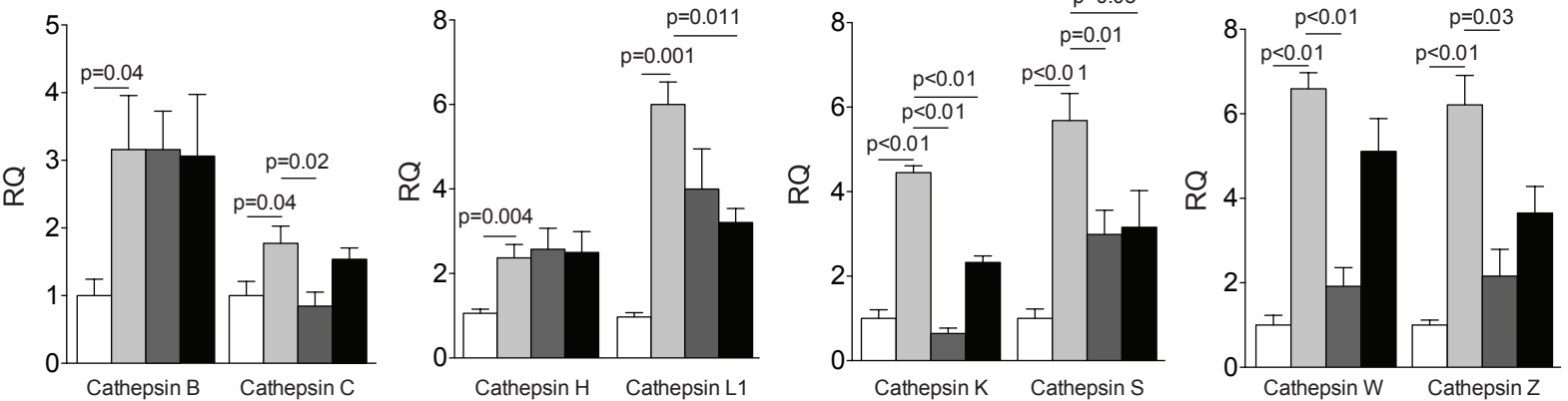
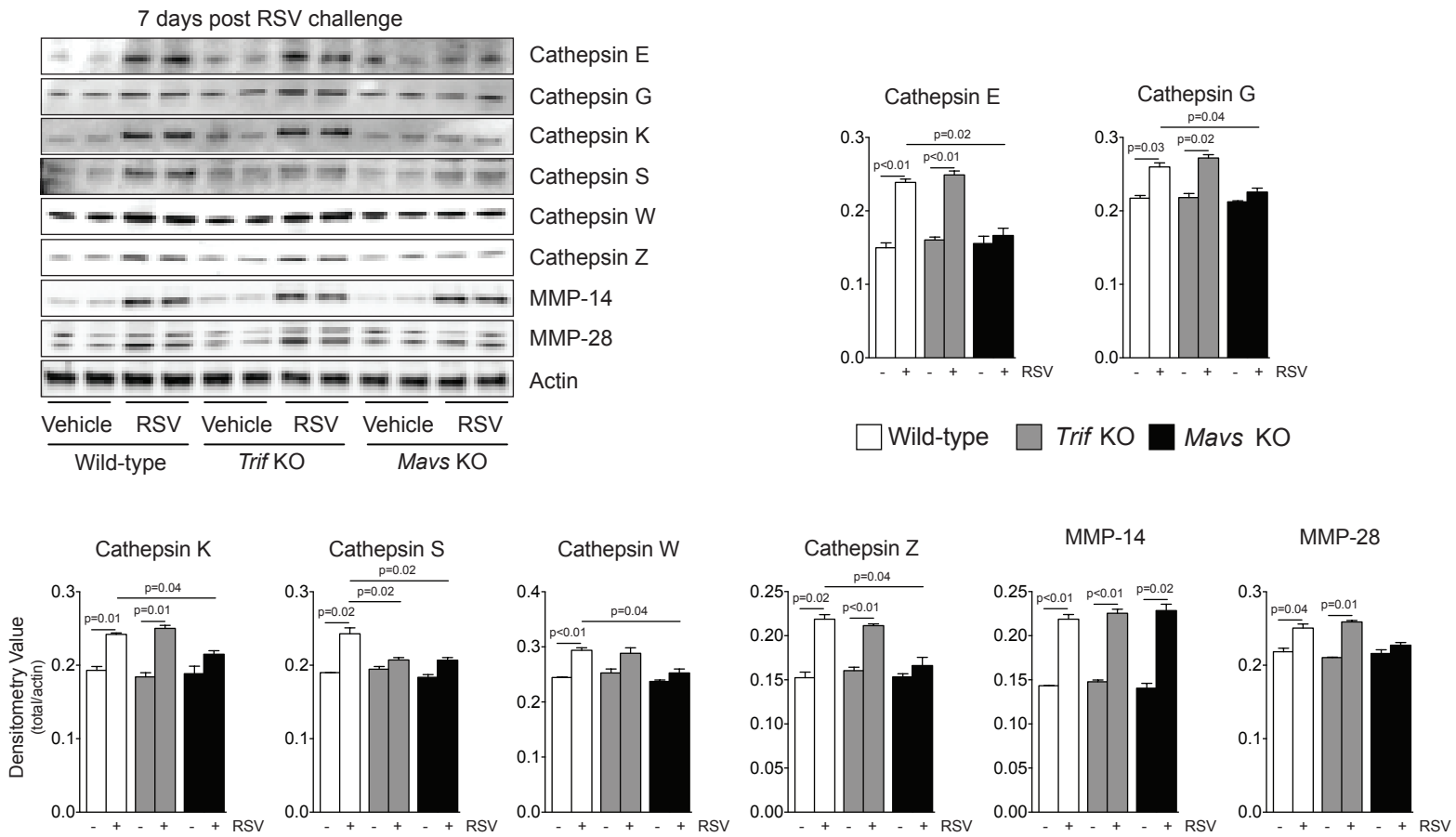


# Figure 6

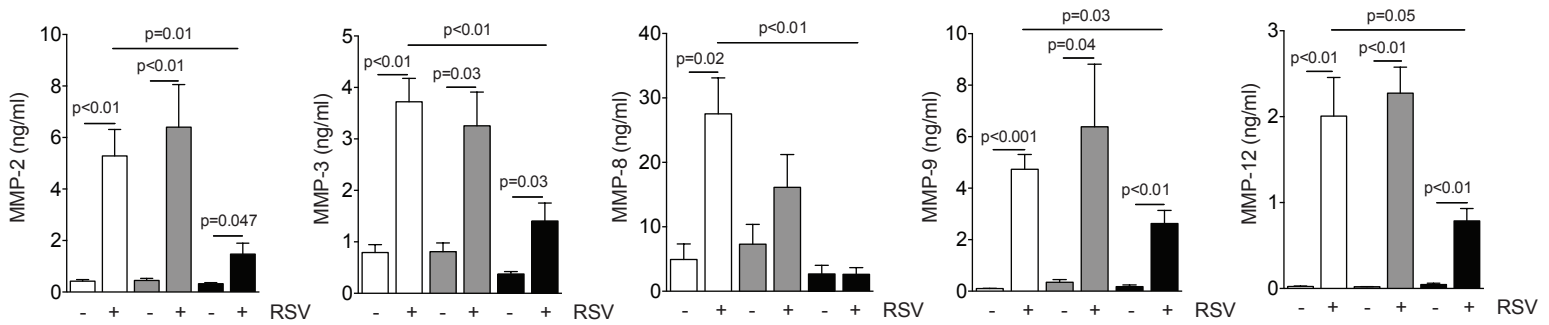
## A



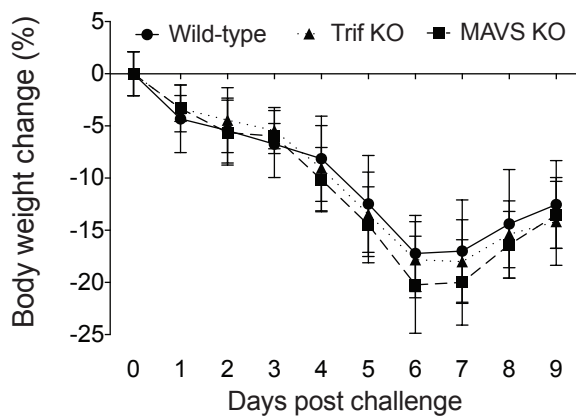
## B

Legend: Wild-type (white bar), *Trif* KO (gray bar), *Mavs* KO (black bar)

7 days post RSV challenge



## C



## D

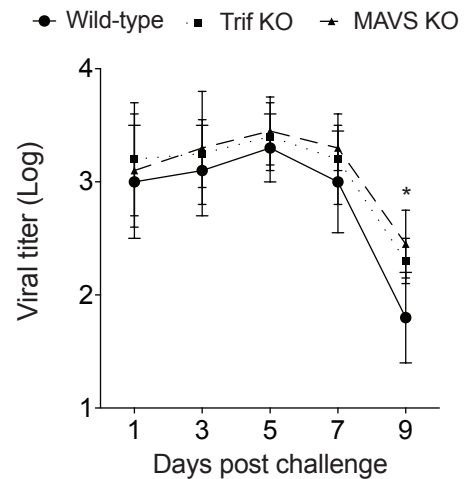




# Figure 7

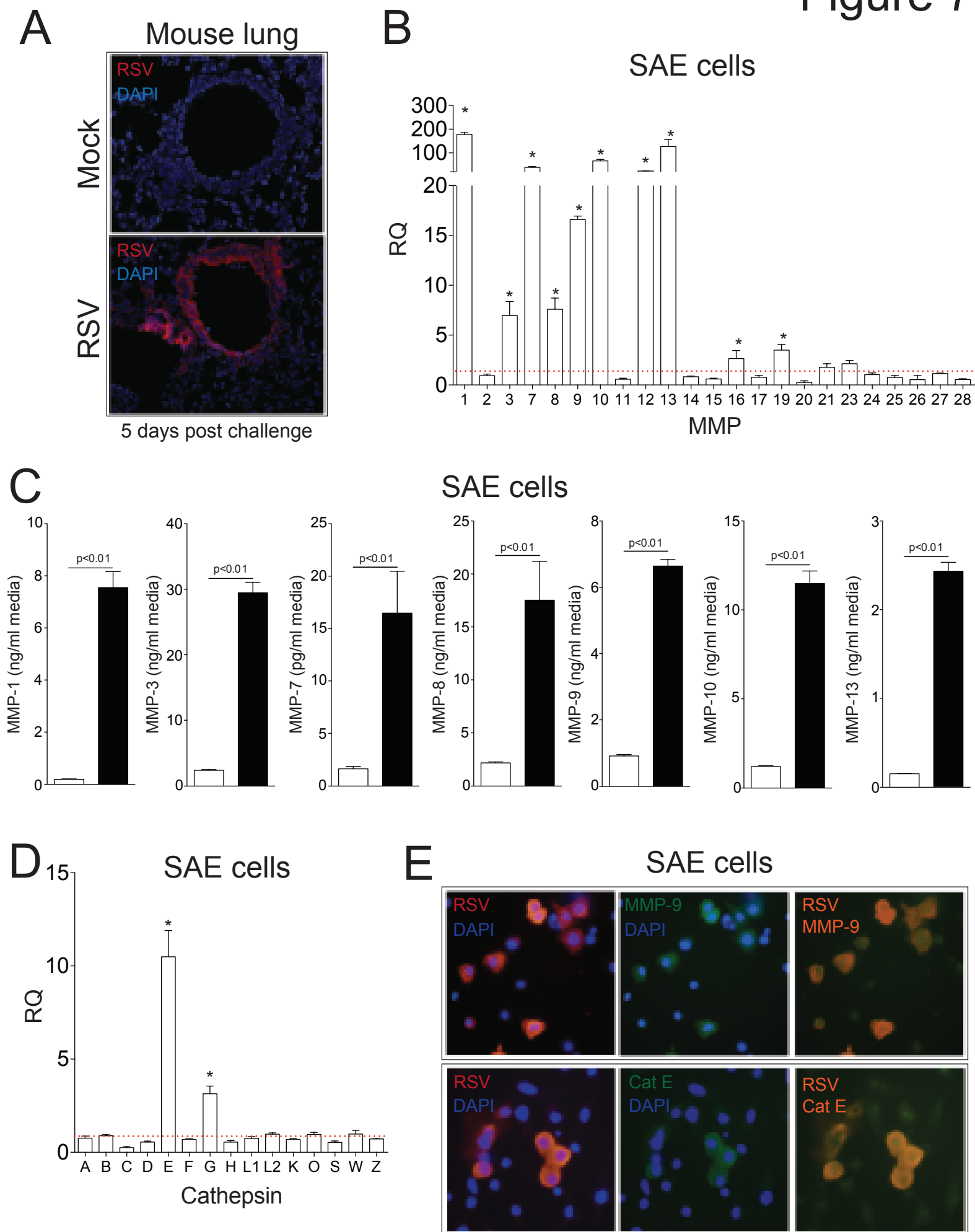


# Figure 8

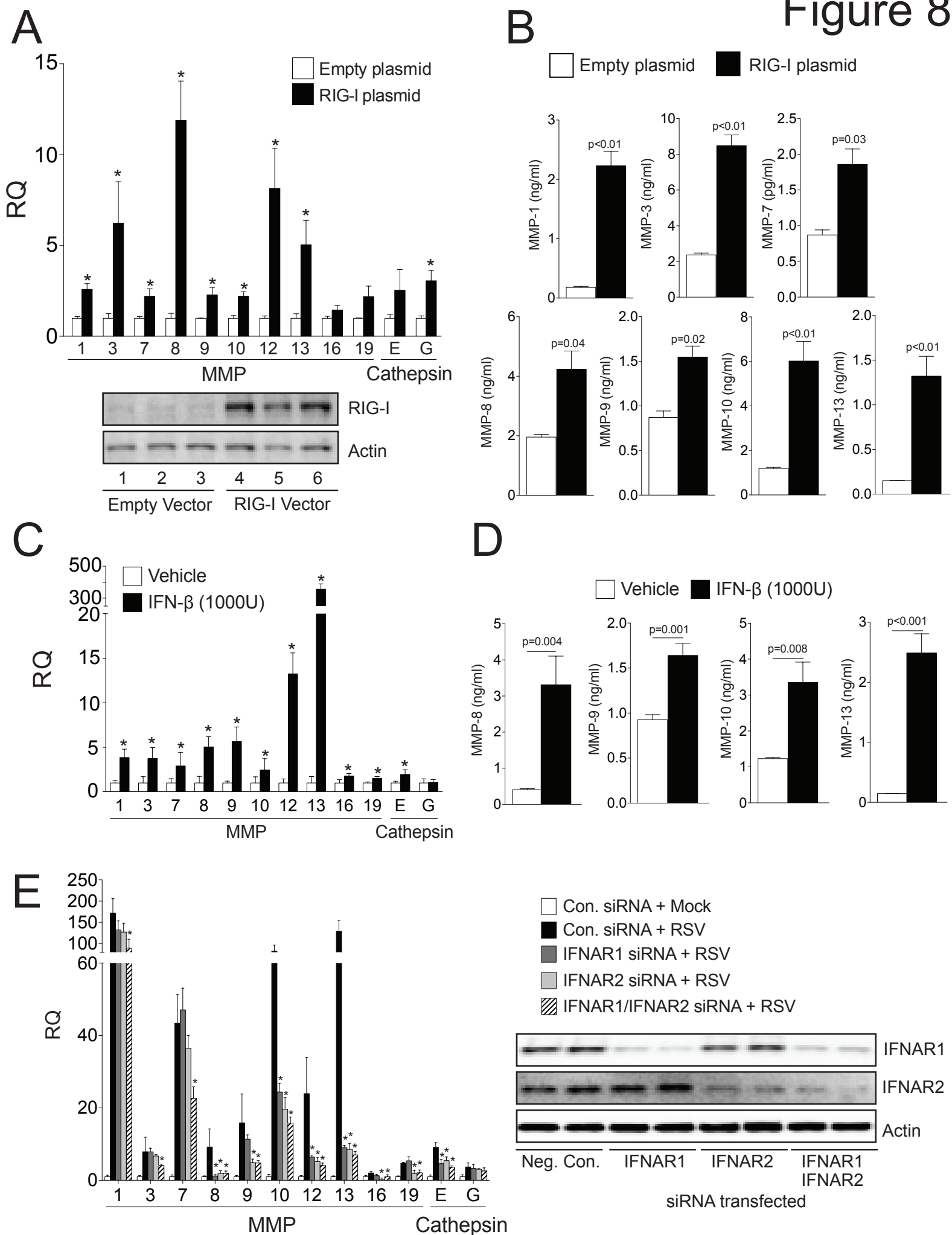
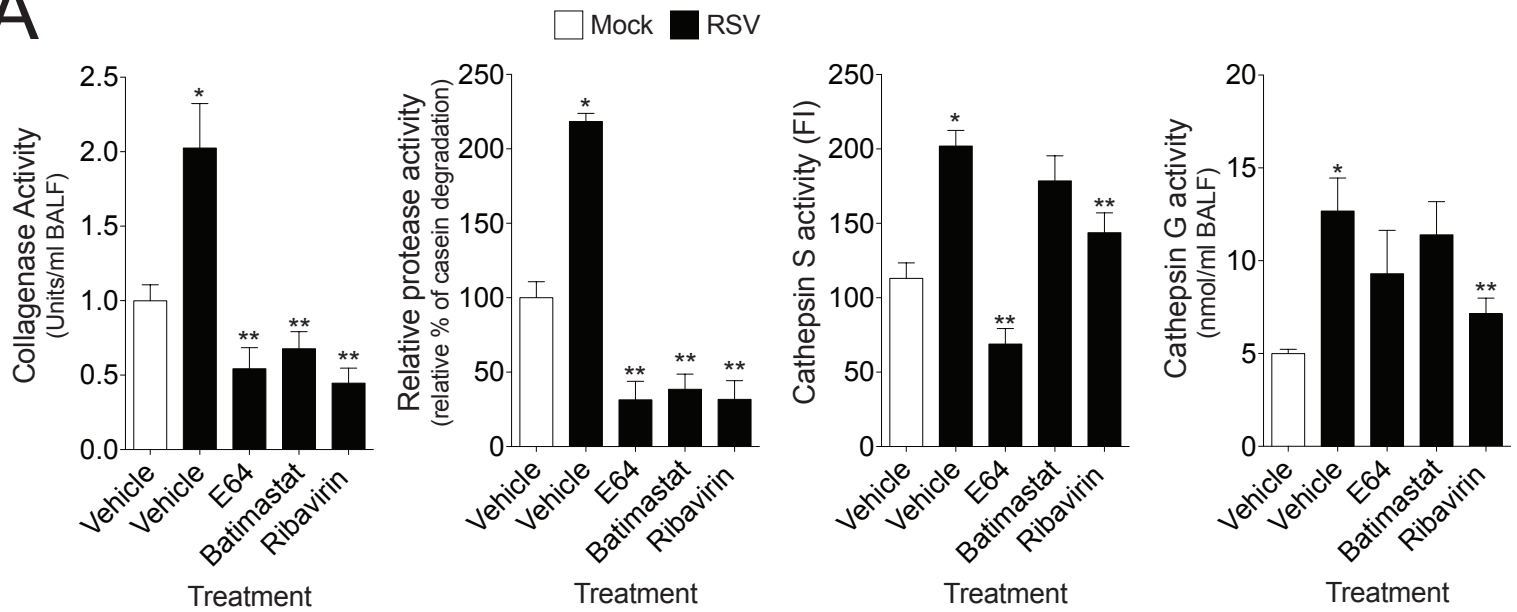
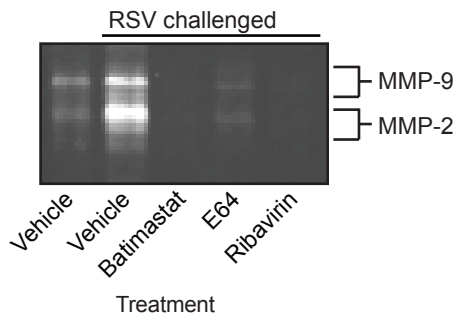


# Figure 9

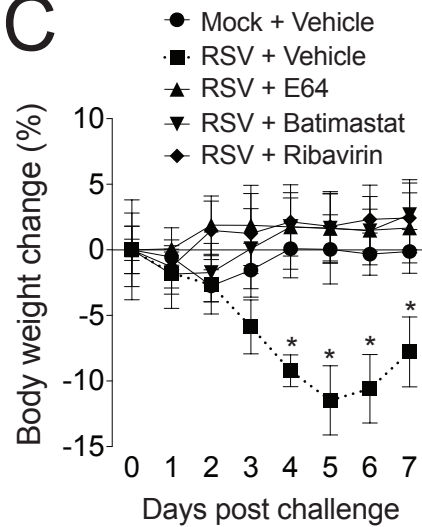
## A



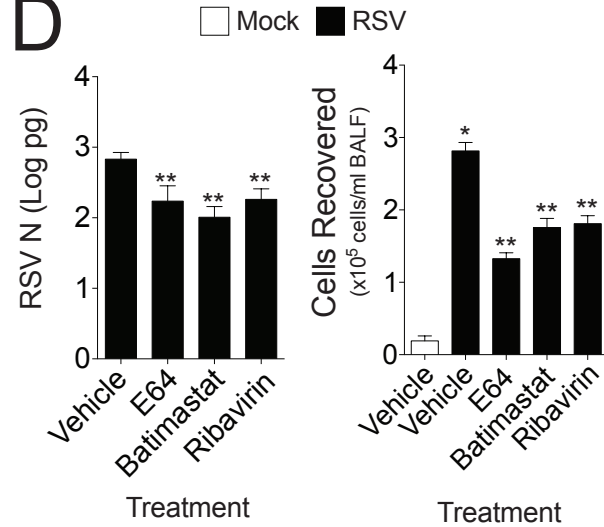
## B



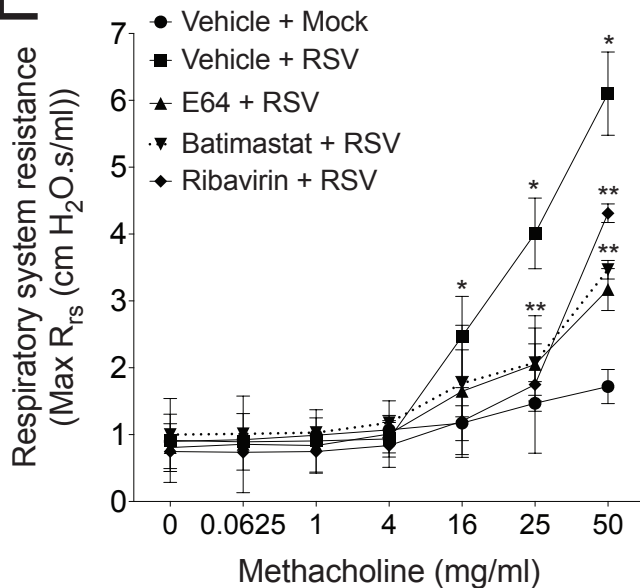
## C



## D



## E



## F

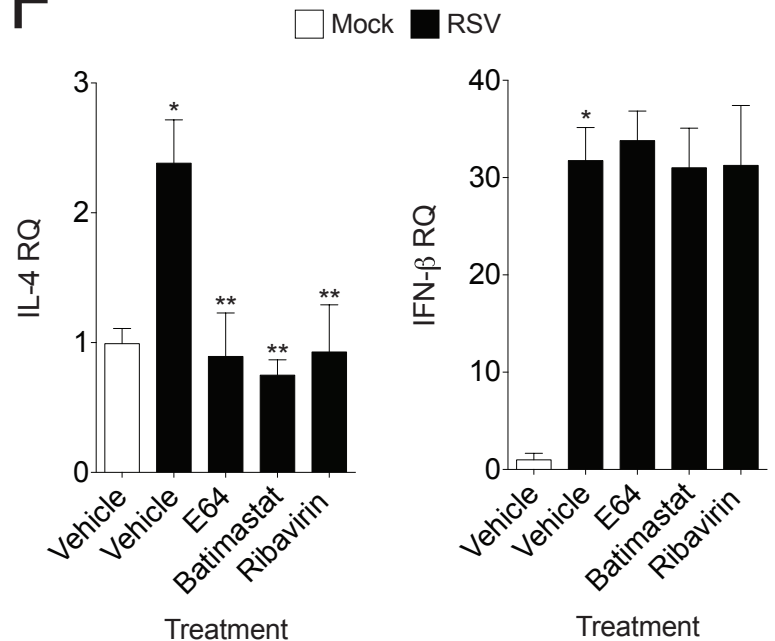
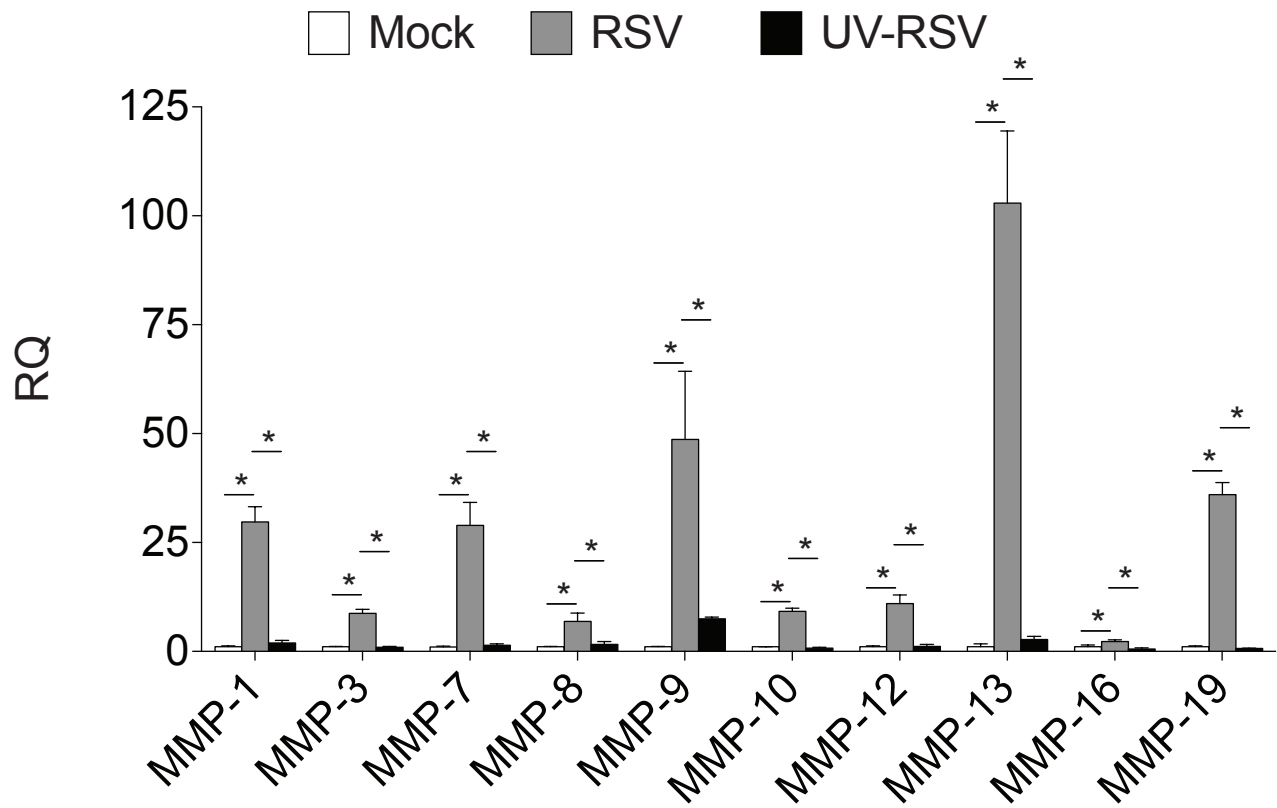


Figure S1

A



B

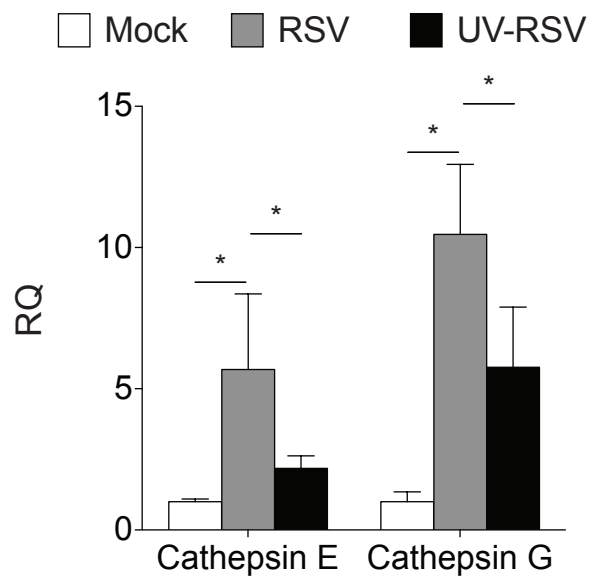
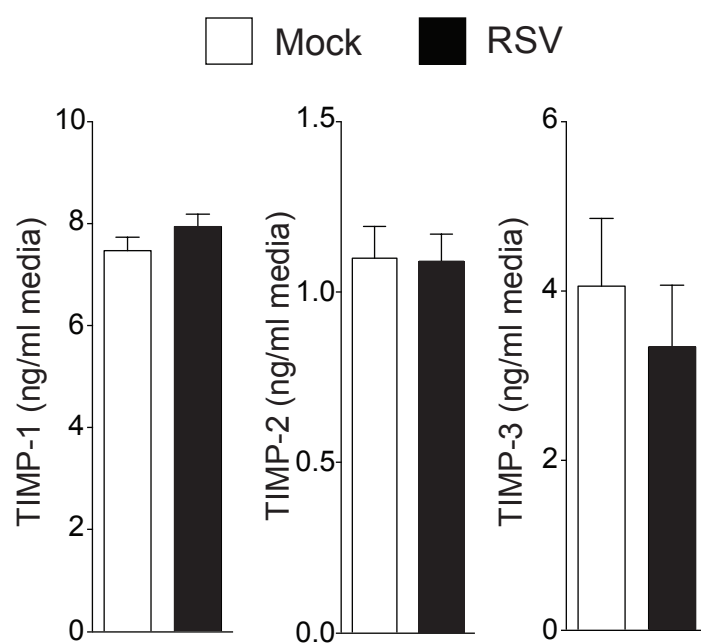


Figure S2



# Figure S3

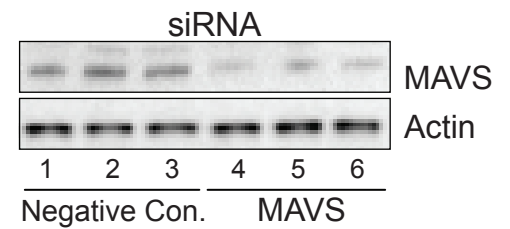
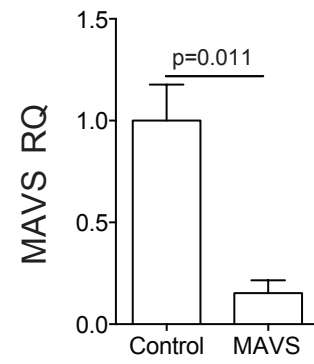
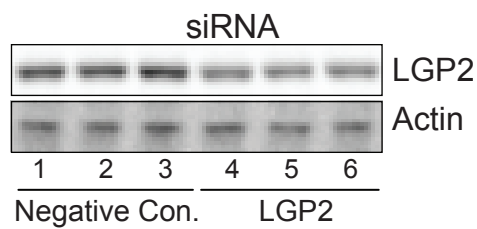
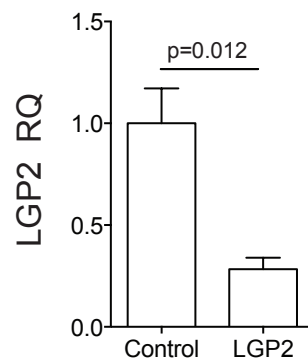
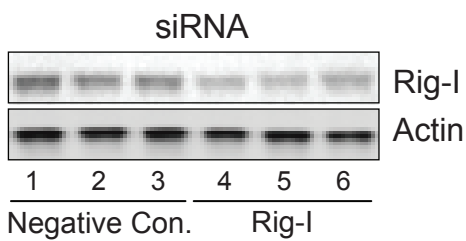
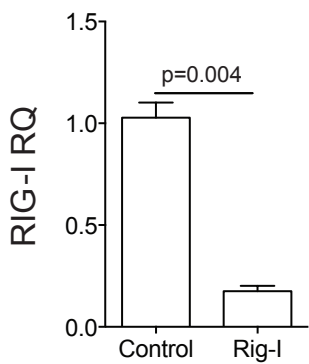
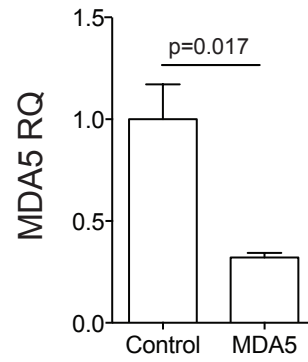
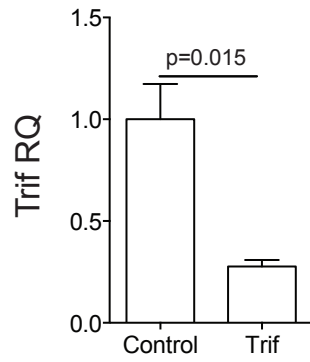
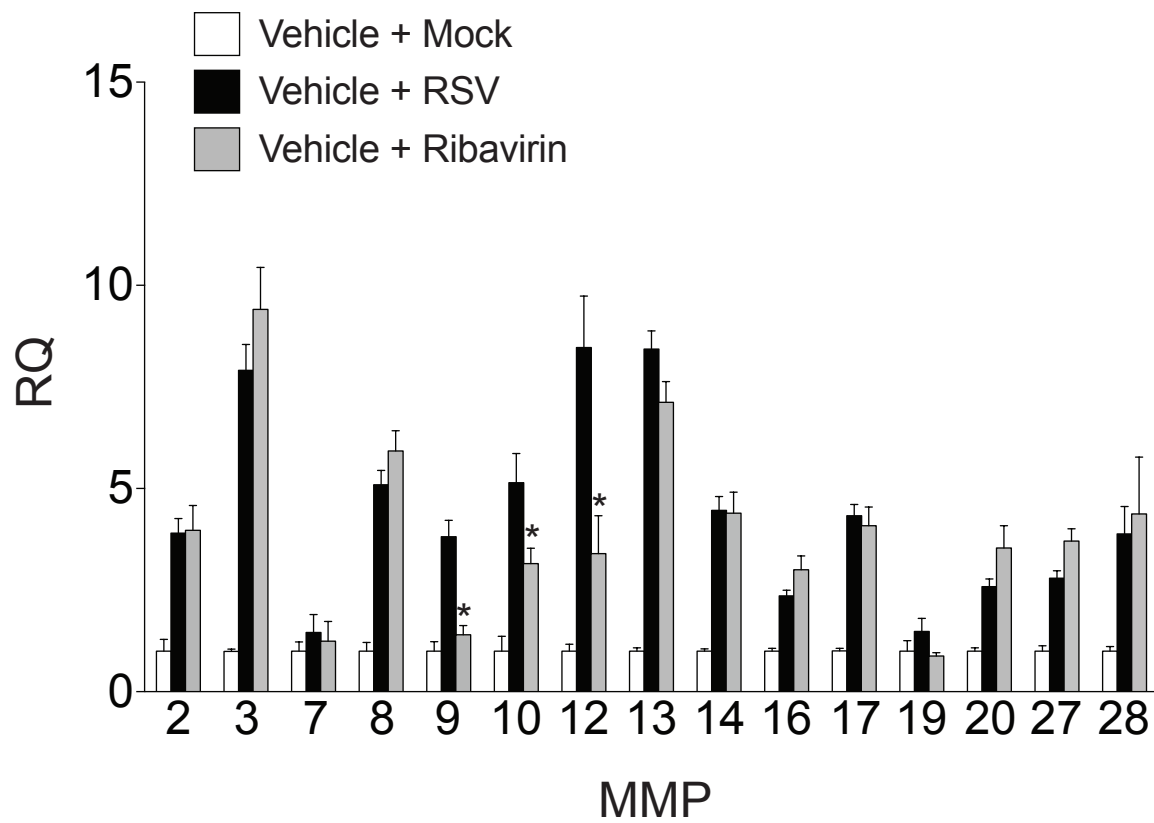


Figure S4

A



B

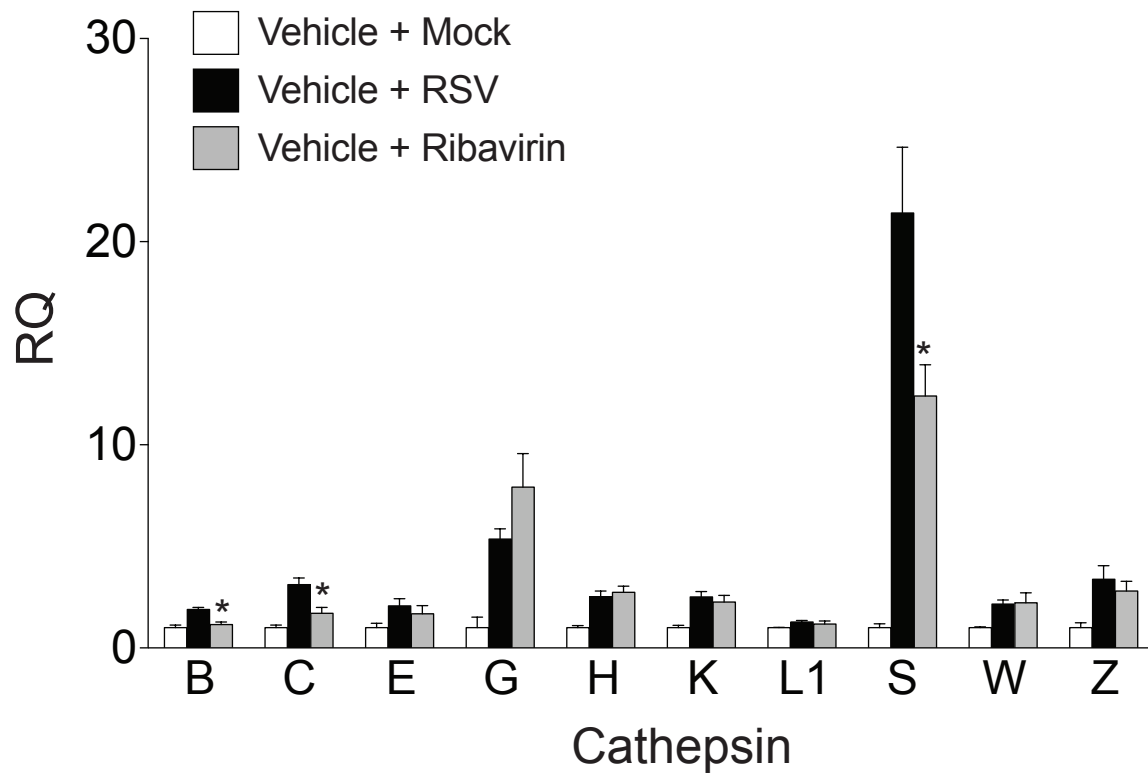
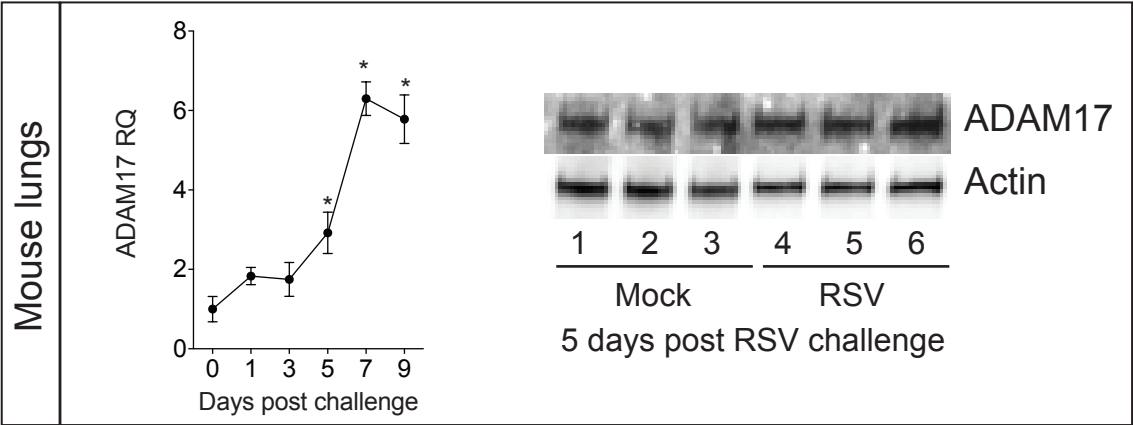


Figure S5

A



B

